Title
PION INTERFEROMETRY OF NUCLEAR COLLISIONS I: THEORY

Author
Gyulassy, M.

Publication Date
1979-04-01

Submitted to Physical Review C

LBL-8759 C.2
Preprint

PION INTERFEROMETRY OF NUCLEAR COLLISIONS I: THEORY

M. Gyulassy, S. K. Kauffmann, Lance W. Wilson

April 1979

Prepared for the U. S. Department of Energy
under Contract W-7405-ENG-48

DISCLAIMER

LBL-8759

PION INTERFEROMETRY OF NUCLEAR COLLISIONS I: THEORY

M. Gyulassy, S. K. Kauffmann, Lance W. Wilson

Nuclear Science Division
Lawrence Berkeley Laboratory
Berkeley, California 94720

ABSTRACT

The topic of pion interferometry (identical pion correlations) is analyzed in detail in the context of relativistic nuclear collisions. Through an exactly solvable field theoretic model specified by an ensemble of classical pion source currents, $J_i(x)$, we calculate the $\pi^-\pi^-$ correlation function, $R(\tilde{k}_1,\tilde{k}_2)$, for chaotic, coherent, and partially coherent pion fields. We analyze how R can be used to determine the degree of coherence of the produced pion field as well as the geometric structure of the source of the chaotic field component. With this model we are able to distinguish between those correlations due to Bose-Einstein symmetrization (the Hanbury Brown and Twiss or Goldhaber effect) and those due to specific multiparticle production dynamics. In particular we show that Bose-Einstein symmetrization dominates the form of $R(\tilde{k}_1,\tilde{k}_2)$ only for chaotic pion fields produced over a time scale large compared to m_π^{-1}. If, due to collective phenomena, there is some coherence of the pion field, then the intercept, $R(\tilde{k},\tilde{k}) = 2 - D^2(\tilde{k})$, is shown to measure mode by mode that degree of coherence $D(\tilde{k})$. Geometric information about the source of the chaotic field component may be extracted from $R(\tilde{k}_1,\tilde{k}_2)$ only after $D(\tilde{k})$ has been determined. Expressions are also derived that incorporate distortions of R due to one-body and two-body final state interactions. These expressions will be numerically evaluated in a subsequent paper. Relative $\pi^-\pi^-$ interactions lead to a

penetration factor, $G(\tilde{k}_1,\tilde{k}_2)$, that modulates the form of $R(\tilde{k}_1,\tilde{k}_2)$. An expression for G is obtained to all orders in the one-body optical potential but first order in the two-body potential. This penetration factor must be evaluated before data for R can be used to determine $D(\tilde{k})$.

Key words: NUCLEAR REACTIONS Relativistic nuclear collisions, multipion inclusive cross sections, $\pi^-\pi^-$ correlations, Hanbury-Brown Twiss effect, partially coherent fields, final state interactions.
PAC: 25.70-z, 24.11.-i, 11.80.-m, 11.10.St, 07.60. Ly

I. INTRODUCTION AND SUMMARY

Pion interferometry involves the study of the correlations between two identical pions (e.g., $\pi^-\pi^-$) produced in hadronic processes. An obvious measure of such correlations can be obtained by comparing the double pion inclusive cross section, $d^6\sigma(\pi^-\pi^-)/d^3k_1 d^3k_3$, to the product of single pion inclusive cross sections, $d^3\sigma(\pi^-)/d^3k$. The precise definition of the correlation function $R(\tilde{k}_1,\tilde{k}_2)$ for negative pions that we consider in this paper is

$$R(\tilde{k}_1,\tilde{k}_2) = \frac{\langle n_{\pi^-}\rangle^2}{\langle n_{\pi^-}(n_{\pi^-}-1)\rangle} \frac{\sigma_{\pi^-}\, d^6\sigma(\pi^-\pi^-)/d^3k_1 d^3k_2}{(d^3\sigma(\pi^-)/d^3k_1)(d^3\sigma(\pi^-)/d^3k_2)} \tag{1.1}$$

where σ_{π^-} is the total negative pion production cross section, and $\langle n_{\pi^-}\rangle$ and $\langle n_{\pi^-}(n_{\pi^-}-1)\rangle$ are the average first and second binomial moments of the π^- multiplicity distribution. The ratio of multiplicity moments in Eq. (1.1) is introduced since the single and double pion inclusive cross sections are normalized as

$$\int d^3k_1 d^3k_2\; d^6\sigma(\pi^-\pi^-)/d^3k_1 d^3k_2 = \langle n_{\pi^-}(n_{\pi^-}-1)\rangle\, \sigma_{\pi^-} \tag{1.2}$$

and

$$\int d^3k_1\; d^3\sigma(\pi^-)/d^3k_1 = \langle n_{\pi^-}\rangle\, \sigma_{\pi^-} \quad . \tag{1.3}$$

The definition of R via Eq. (1.1) insures that $R \equiv 1$ if the negative pions are uncorrelated in momentum space [i.e., $d^6\sigma(\pi^-\pi^-)/d^3k_1 d^3k_2 \propto f(\tilde{k}_1)f(\tilde{k}_2)$] regardless of whether the π^- multiplicity distribution is Poisson or not. The correlation function for positively charged pion pairs is defined similarly to Eq. (1.1).

The term "pion interferometry" is used to emphasize the analogy that the study of pion correlations via Eq. (1.1) has to the well known technique of second order *intensity interferometry*[1] developed by Hanbury-Brown and Twiss to measure stellar radii. In quantum scattering theory the application of intensity interferometry to deduce structural properties of the target was formalized by Goldberger, Lewis and Watson.[2] Later, the idea of using intensity interferometry with pions to deduce the space-time structure of high energy hadronic processes was developed by Kopylov and Podgoretsky,[3] Shuryak,[4] and Cocconi.[5]

Experimentally, pion interferometry was first used by Goldhaber, Goldhaber, Lee and Pais[6] (GGLP) to determine the dimensions of the pion production region in $\bar{p}p$ annihilation. They suggested that intensity interferometry is a consequence of the Bose-Einstein symmetrization required for two identical pions. In fact, the enhancement of $R(\tilde{k}_1,\tilde{k}_2)$ in Eq. (1.1) above 1 for small relative momenta has sometimes been referred to as the GGLP effect. Pion interferometry has also been applied to other processes such as πp, pp, Kp collisions[7-11] to determine the space-time dimensions of the pion source. The most recent and extensive experimental analysis of pion correlation data based on pion interferometry is given in Ref. 12.

The most exciting recent theoretical development has been the observation[13-15] that not only can the study of pion correlations reveal the space-time structure of the pion production region, but also $R(\tilde{k}_1,\tilde{k}_2)$ can provide information on the degree of coherence of the produced pion field. Thus $R(\tilde{k}_1,\tilde{k}_2)$ could ideally provide both geometrical and dynamical information on pion production in a given reaction.

It is therefore natural that these ideas on pion interferometry have also found their way[16,17] into the field of relativistic (~1 GeV/nucleon) nuclear collisions. Since many of the models for nuclear collisions[18] involve classical geometrical concepts (e.g., classical trajectories, impact parameters), the determination of the space-time structure of the pion source region could in principle provide valuable constraints on these models. For example, the dimensions and lifetime of the pion production region as calculated with either intranuclear cascade or hydrodynamic models could then be compared to data. However, in addition to such geometrical information,[17] the pion correlation function $R(\tilde{k}_1,\tilde{k}_2)$ could ideally shed light on possible exotic processes that may also be involved in nuclear collisions.[16]

We note that the first data on pion interferometry in nuclear collisions ($^{40}Ar + Pb_3O_4 \rightarrow \pi^-\pi^- + X$ at 1.8 GeV/nucleon) are now available[19] and clearly demonstrate the feasibility of such studies. Furthermore, future experiments[20] using the Bevalac at the Lawrence Berkeley Laboratory are expected to increase significantly the amount of data on the two pion correlations.

The purpose of this work is therefore to analyze in detail the topic of pion interferometry in the context of nuclear collisions. At the same time we will discuss and attempt to clarify the theory of pion interferometry as applied to any hadronic process. In this paper we concentrate on the interplay between the pion production and final state dynamics and Bose-Einstein symmetrization in determining the form of $R(\tilde{k}_1,\tilde{k}_2)$. In particular, we focus on the difference between chaotic and coherent pion fields and how the degree of coherence affects $R(\tilde{k}_1,\tilde{k}_2)$. In a

subsequent paper,[21] we will apply the formalism developed in Sections IV and V to obtain numerical estimates of the effects of final state interactions on pion correlations in nuclear collisions and to discuss specific experimental problems.

We now summarize the results obtained in the following sections. In Section II, we discuss the various competing sources of pion correlations in hadronic processes with special attention given to nuclear collisions. The role of Bose-Einstein symmetrization on the ideal correlation function (the GGLP effect) is then reviewed in Section III. The usual heuristic derivations of the form of the correlation function are presented and criticized because they neglect effects of multiparticle dynamics on R. To enable us to incorporate such effects we develop next in Section IV a density matrix formalism for calculating $R(\tilde{k}_1,\tilde{k}_2)$. The density matrix is parametrized via an ensemble of coherent pion states, $|J\rangle$, produced by an ensemble of classical (c-number) source currents $J(x)$. In Section IV.C, we show how such an ensemble of currents arises from a space-time picture of pion production involving isolated inelastic scattering centers. We analyze in detail the single and double inclusive distribution and show that multipion production amplitudes lead to interference terms in $R(\tilde{k}_1,\tilde{k}_2)$ that are, in general, much more complex than those obtained from Bose-Einstein symmetrization alone in Section III. We find that the necessary conditions for $R(\tilde{k}_1,\tilde{k}_2)$ to reduce to the ideal Bose-Einstein form are that the number of independent source currents is very large and that the total interaction time be large compared to m_π^{-1}. Those conditions are shown in Section IV.C.2 to lead to the production of chaotic pion fields. In Section IV.D, the

effects of possible collective pion production mechanisms are calculated. We derive the form of $R(\tilde{k}_1,\tilde{k}_2)$, Eq. (4.66), for the case of partially coherent fields that can arise when a group of nucleons radiate pions collectively. Equation (4.66) shows exactly how $R(\tilde{k}_1,\tilde{k}_2)$ can determine the degree of coherence of the pion field as well as the geometrical structure of the source of the chaotic component. The intercept $R(\tilde{k},\tilde{k}) = 2 - D^2(\tilde{k})$ determines, in the absence of final state interactions, the degree of coherence $D(\tilde{k})$, i.e., fraction of pions with momentum $\tilde{k}$ in the coherent state component. Finally, in Section V we calculate how final state interactions distort the form of $R(\tilde{k}_1,\tilde{k}_2)$. In Section V.B, the exactly solvable field theoretic model, Eqs. (5.1) and (5.6), is presented showing how arbitrary one-body optical potentials V(x) distort $R(\tilde{k}_1,\tilde{k}_2)$ via Eq. (5.36). In Section V.C, an approximate treatment of two-body final state interactions, U(x-y), is presented in terms of Bethe-Salpeter amplitudes. The effect of U(x-y) is shown in Eq. (5.52) to lead to a Gamow penetration factor that modulates the form of $R(\tilde{k}_1,\tilde{k}_2)$. Our most general result for R is Eq. (5.63) incorporating distortions to all orders in V and first order in U, and applicable for partially coherent fields.

The complexity of final state interaction distortions displayed in Eq. (5.63) demonstrates that the naive analysis of correlation data via Eq. (3.6) or (4.67) even for chaotic fields may lead to inaccurate geometrical and dynamical information. For example, two-body $\pi^-\pi^-$ final state interactions can simulate a finite degree of coherence and one body optical potentials can lead to 100% distortions of the apparent geometry of the chaotic source.[21] A systematic numerical study to be

reported in Ref. 21 of the expression obtained here has shown that final state distortions are sensitive to the magnitude of the mean momentum $k = (\tilde{k}_1 + \tilde{k}_2)/2$ of the observed pion pair as well as to the orientation of $\tilde{q} = \tilde{k}_1 - \tilde{k}_2$ with respect to $\tilde{k}$. The most ideal configuration to study experimentally is $\tilde{k}\cdot\tilde{q} = 0$, i.e., equal energy pions, because this configuration is found to be the least sensitive to uncertainties in the one body optical potential. Furthermore, optical potential distortions can be minimized by concentrating on high momentum $|\tilde{k}| > m_\pi$ pion pairs. By measuring $R(\tilde{k}_1,\tilde{k}_2)$ as a function of $\tilde{q}$ for fixed large $\tilde{k}$ such that $\tilde{q}\cdot\tilde{k} = 0$, it should be possible to unfold final state distortion from correlation data.

Note that throughout this paper we use natural units, $\hbar = c = 1$.

II. GENERAL REMARKS ON PION CORRELATIONS

Correlations between identical pions produced in hadronic processes can arise from a combination of several sources:

1) Conservation laws:
   energy momentum
   quantum numbers
2) Dynamics:
   production dynamics
   final state interactions
3) Bose-Einstein statistics

There are basically two types of conservation laws: those associated with kinematics and those associated with internal symmetries or quantum numbers. The conservation of energy-momentum leads to kinematic constraints between the produced particles and leads to strong correlations when one pion is observed with a momentum near a kinematic boundary. For example, if one pion carries away a large fraction of the available center of mass energy, then a strong anticorrelation must be observed ($R(\tilde{k}_1,\tilde{k}_2) << 1$ for $\tilde{k}_2 \approx \tilde{k}_1$ when $|\tilde{k}_1| \to k_{max}$). Such kinematic correlations can of course be evaluated from Lorentz Invariant Phase Space (LIPS) integrals (see, e.g., Ref. 22).

Conservation of internal symmetries and quantum numbers such as isospin and parity lead to correlations between the number of different charged pions that can be produced in a given reaction. Therefore, such constraints affect mainly the pion multiplicity distributions and, hence, the binomial moments in Eqs. (1.1)-(1.3). An example of such multiplicity correlations is given in Ref. 23. To isolate the true *momentum space correlations* with $R(\tilde{k}_1,\tilde{k}_2)$, it is therefore necessary to remove the

dependence of the normalization of R on the specific multiplicity distribution. The correlation function as defined in Eq. (1.1) accomplishes this goal. For an independent pion emission mechanism,[23] $R \equiv 1$ regardless of the constraints imposed on $\langle n_{\pi^-} \rangle$ and $\langle n_{\pi^-}(n_{\pi^-} - 1) \rangle$ by internal symmetries. It should be noted that $\langle n_{\pi^-} \rangle^2 = \langle n_{\pi}(n_{\pi} - 1) \rangle$ when the multiplicity distribution has a Poisson form, as seems to be the case for fixed impact parameters in nuclear collisions.[24]

Besides correlations induced by conservation laws, it is clear that the specific pion production mechanism as well as the interactions of the produced pions with other hadrons in the final state can also lead to pion correlations. The most obvious example of a production mechanism that leads to correlations is resonance production[25,26] (e.g., ρ, A_1, etc.). Another dynamical production model that leads to strong correlations is the cluster model[15] in which pions and resonances arise as decay products of hadronic clusters (fireballs) that are independently produced in a hadronic collision. In Ref. 15 the cluster model provides an interesting example of how dynamical, kinematical, and symmetry constraints can all play major roles in influencing pion correlations. In contrast to this model, there are also dynamical models that lead to *no* intensity correlations. As discussed in Ref. 23 and noted in Ref. 4, a classical bremsstrahlung model for pion production leads to coherent states which exhibit no pion intensity correlations and, hence, no Hanbury-Brown, Twiss (or GGLP) effect. Recently, Fowler and Weiner[13] have also emphasized this point. In addition, the role of coherent vs. incoherent emission processes in influencing pion correlations has been discussed in Ref. 14 from a topological approach to hadron dynamics. It is

in fact precisely this sensitivity to pion production dynamics that makes the study of pion correlations so attractive in our view.

There is, however, another dynamical source of correlations that stands in the way of simple analysis of correlation data: namely, final state interactions. While there is no rigorous separation between production dynamics and final state interactions, an approximate distinction can be made (see Section V). The best example of this is the long-range Coulomb interaction that exists between the final hadrons for times long after the hadrons have been produced and are out of the range of strong interactions. Normally, we think of Coulomb interactions as small perturbations to strong interactions. However, correlations between hadrons with small relative momentum ($q \lesssim m_\pi\sqrt{\alpha}$) can be completely dominated by Coulomb effects. In the case of nuclear collisions, Coulomb distortions extend to even larger relative momentum, $q \lesssim (Z\alpha m_\pi/R)^{\frac{1}{2}} \sim Z^{\frac{1}{3}}(m_\pi\sqrt{\alpha})$. The correlations induced by such final state interactions can therefore completely mask or distort the correlations (or non-correlations) resulting from particular *production* dynamics. Clearly, the extent to which we can deduce various aspects of the production dynamics from correlation measurements depends on our ability to untangle the distortions due to final state interactions.

The sources of correlations discussed so far apply to any pair of hadrons in the final state. However, there is yet another source of correlations when the two hadrons are indistinguishable -- Fermi-Dirac (FD) or Bose-Einstein (BE) statistics. For identical pions ($\pi^-\pi^-$), BE statistics will obviously lead to enhanced correlations ($R(q) > 1$) for small relative momenta q (the GGLP effect[6]). On the other hand, for

identical fermions (pp), FD statistics will lead to anticorrelations ($R(q) < 1$) for small q. However, it must always be remembered that such correlations can be significantly modified by the other sources of correlations mentioned above. Whether the GGLP effect dominates $R(\tilde{k}_1,\tilde{k}_2)$ will depend strongly on the particular reaction under study.

In the case of relativistic nuclear collisions, a typical reaction of interest is[19]

$$^{40}Ar + Pb_3O_4 \rightarrow \pi^-\pi^- + X \qquad (2.1)$$

for an Ar beam with 1.8 GeV/nucleon lab kinetic energy. For a reaction with Pb the total *center of mass* kinetic energy available for pion production is $\sqrt{s} - M_{Ar} - M_{Pb} \approx 54$ GeV. Therefore the number of pions that are kinematically allowed (but with vanishing probability) is $n_\pi(\max) \approx 386$! In fact,[24,27] the number of negative pions observed in reaction (2.1) ranges between 1-15 with average energies in the range ~10-200 MeV in the center of mass. Therefore, there are not expected to be any significant kinematic correlations for pion pairs in such reactions. Furthermore, quantum number constraints such as charge and parity conservation should also lead to negligible pion correlations because of the "reservoir" of quantum numbers provided by the 102 protons and 146 neutrons in the initial nuclear state. Therefore, we expect conservation laws to have little effect on $R(\tilde{k}_1,\tilde{k}_2)$ for nuclear collisions.

Next, consider dynamical correlations. The dynamics of reactions such as Eq. (2.1) are expected to be dominated by multiple nucleon-nucleon collisions[18,32] (nucleon cascading), where the relevant input quantities are the nucleon-nucleon cross sections in the 1-2 GeV range.

Therefore, multipion resonance (ρ, ω, ...) production is infrequent, and the main source of pions is through $\Delta_{33}(1232)$ production and decay. Since the pions in the nuclear cascade model are produced singly at random space-time points with possibly many subsequent rescatterings in the nuclear system, the pion field is expected to be chaotic[1,17] in such a model. Nevertheless, exotic production dynamics due to collective nuclear instabilities could possibly also occur in relativistic nuclear collisions.[16,28] If pionic instabilities[28] do in fact occur and lead to a coherent pion field admixture in the final state, then $R(\tilde{k}_1,\tilde{k}_2)$ could provide evidence for such phenomena.[13,16] The form of R for partially coherent fields is derived in Section IV.D. However, as noted before, the effects of final state interactions must be unfolded from $R(\tilde{k}_1,\tilde{k}_2)$ before such an analysis is possible. In the reaction (2.1), the typical residual nucleon charge is $Z \sim 100$ and major distortions of $R(\tilde{k}_1,\tilde{k}_2)$ can be expected[21] for $|\tilde{k}_1-\tilde{k}_2| \lesssim 50$ MeV/c.

In summary, dynamical correlations are expected to influence pion correlations in nuclear collisions only through final state interactions if the cascade picture for pion production holds. On the other hand, both production and final state dynamics will affect R if exotic phenomena occur. In any case, conservation laws are expected to have negligible effect on R for nuclear collisions.

Bose-Einstein statistics of course must always be taken into account. However, BE interference will dominate R only if no exotic phenomena occur and final state interactions can be shown to be small (see Ref. 21).

We turn next to the special case when BE interference dominates the $\pi^-\pi^-$ correlation function.

III. IDEAL BOSE-EINSTEIN INTERFERENCE

The usual derivation[2,5,6] of the GGLP effect begins with the observation that the amplitude, Ψ_{12}, for observing two identical pions with momenta $\tilde{k}_1$ and $\tilde{k}_2$ given that they were produced at points $\tilde{x}_1$ and $\tilde{x}_2$ is given by

$$\Psi_{12} = \langle \tilde{k}_1 \tilde{k}_2 | \tilde{x}_1 \tilde{x}_2 \rangle \propto \frac{1}{\sqrt{2}} \left\{ e^{-i\tilde{k}_1\tilde{x}_1} e^{-i\tilde{k}_2\tilde{x}_2} + e^{-i\tilde{k}_1\tilde{x}_2} e^{-i\tilde{k}_2\tilde{x}_1} \right\} , \tag{3.1}$$

where the second term in Eq. (3.1) arises, of course, from the symmetrization required by BE statistics. The second step is to assume that the pion source points $\tilde{x}_1$ and $\tilde{x}_2$ are randomly distributed in a region of space specified by a normalized density distribution, $\rho(\tilde{x})$. Then the probability of observing two identical pions with momenta $\tilde{k}_1$ and $\tilde{k}_2$ is obtained via

$$P(\tilde{k}_1,\tilde{k}_2) \propto \int d^3x_1 d^3x_2 \; \rho(\tilde{x}_1)\rho(\tilde{x}_2)|\Psi_{12}|^2 \propto 1 + |\rho(\tilde{k}_1 - \tilde{k}_2)|^2 , \tag{3.2}$$

where $\rho(\tilde{q})$ is the Fourier transform of $\rho(\tilde{x})$. The second term in Eq. (3.2) is the consequence of the BE interference between the two parts of the amplitude in Eq. (3.1). From Eq. (3.2) we therefore expect $R(\tilde{k}_1,\tilde{k}_1-\tilde{q}) \propto P(\tilde{q})$ to measure the absolute square of the Fourier transform $|\rho(\tilde{q})|^2$, of the pion source distribution.

To incorporate also the time dependence of the pion source, Kopylov and Podgoretsky[3] derived the form of $R(\tilde{k}_1,\tilde{k}_2)$ using the first quantized Klein-Gordon equation in the presence of several source currents, $J_i(\tilde{x},t)$.

The amplitude $\phi_i(\tilde{x},t)$ for a single pion to be found at $(\tilde{x},t)$, given that it was produced by source $J_i(\tilde{x},t)$, was calculated in Ref. 3 from

$$(\partial_\mu \partial^\mu + m_\pi^2)\ \phi_i(\tilde{x},t) \ = \ J_i(\tilde{x},t) \qquad . \tag{3.3}$$

By parametrizing the source currents as

$$J_i(\tilde{x},t) \ = \ J(\tilde{x} - \tilde{x}_i,\ t - t_i) \qquad , \tag{3.4}$$

where the "centers" $(\tilde{x}_i,t_i)$ were assumed to be randomly distributed according to a *space-time* distribution $\rho(x) \equiv \rho(\tilde{x},t)$, the amplitude for observing two pions with momenta $\tilde{k}_1$ and $\tilde{k}_2$ was constructed as

$$\begin{aligned} \Psi_{12} \ &= \ \frac{1}{\sqrt{2}} \left\{ \phi_1(\tilde{k}_1,\omega_1)\phi_2(\tilde{k}_2,\omega_2) + \phi_1(\tilde{k}_2,\omega_2)\phi_2(\tilde{k}_1,\omega_1) \right\} \\ &\propto \ \frac{1}{\sqrt{2}} \left\{ e^{ik_1x_1}\, e^{ik_2x_2} + e^{ik_1x_2}\, e^{ik_2x_1} \right\} \mathcal{J}(k_1)\, \mathcal{J}(k_2) \ , \end{aligned} \tag{3.5}$$

where $k_i x_j = \omega_i t_j - \tilde{k}_i \tilde{x}_j$, and where $\mathcal{J}(k) = J(k)\Delta_\pi(k)$, with $J(k)$ being the space-time Fourier transform of $J(\tilde{x},t)$, and $\Delta_\pi(k) = (k^2 - m^2 + i\varepsilon)^{-1}$ being the pion propagator. Assuming $J(x) = \delta^4(x)$ and ignoring the problem associated with the on-shell singularity of $\Delta_\pi(k^2 = m_\pi^2) = \infty$, Ref. 3 finally obtained

$$R(\tilde{k}_1,\tilde{k}_2) \ \propto \ 1 + \left|\rho(\tilde{k}_1 - \tilde{k}_2,\ \omega_1 - \omega_2)\right|^2 \qquad . \tag{3.6}$$

This heuristic derivation suggested then that R measures not only the space but also the time Fourier transform of $\rho(\tilde{x},t)$. Equation (3.6) is the basis of the expectation that the intensity interference pattern measured via $R(\tilde{k}_1,\tilde{k}_2)$ in Eq. (1.1) can (ideally) be used to deduce the

space-time structure of the pion source .

In actual applications the parametrization that is used most often to determine a radius, R_o, and a lifetime, τ_o, of the pion source is[3,7,8,9,11,12]

$$R(q_o,q_t) \propto 1 + \frac{I^2(q_t R_o)}{1 + (q_o\tau_o)^2} \quad , \tag{3.7}$$

where the Kopylov variables are defined as

$$q_o = \omega_1 - \omega_2$$

$$q_t = \frac{|(\tilde{k}_1-\tilde{k}_2) \times (\tilde{k}_1+\tilde{k}_2)|}{|\tilde{k}_1 + \tilde{k}_2|} \quad , \tag{3.8}$$

and $I(x) = 2J_1(x)/x$, where J_1 is the first order Bessel function. Equation (3.7) follows for a uniform radiating disc of radius R_o oriented in direction $\hat{n} = (\tilde{k}_1+\tilde{k}_2)/|\tilde{k}_1+\tilde{k}_2|$, and having lifetime τ_o, i.e.,

$$\rho(\tilde{x},t) = \{\delta(\tilde{x}\cdot\hat{n})\theta\left(R_o^2 - (\tilde{x} - (\tilde{x}\cdot\hat{n})\hat{n})^2\right)/\pi R_o^2\}\ \{\theta(t)\ e^{-t/\tau_o}/\tau_o\} \ . \tag{3.9}$$

Another parametrization that is sometimes convenient involves a Gaussian form for the space-time distribution.[2,10,17,19] In practice though, the parameters R_o and τ_o do not differ significantly when obtained via Eq. (3.7) or its Gaussian analog.[19]

Having thus reviewed the usual derivations of the GGLP effect, it is important to note several deficiencies in these. First, there is the question of normalization. The use of plane waves and free pion propagators in Eq. (3.5) clearly leads to divergences which are hard to treat in a rigorous manner. A second more serious criticism is that these

derivations do not properly address the multiparticle nature of the final hadronic state. Only two-particle pion wavefunctions ψ_{12} are considered, although in general, a coherent superposition of multipion wavefunctions (and hence, a nontrivial multiplicity distribution) must describe the final hadronic state. Given the source term, Eq. (3.3) must be considered as a *field* equation and cannot be justified as a first quantized wave equation. Thirdly, a specific dynamical assumption has been made in Eq. (3.5) whereby pions are produced independently at random space-time points. Such a derivation therefore cannot reveal the effects of possible coherent pion production dynamics.[13,14,16] Fourth, in actual applications, Eq. (3.7) is still not general enough even for chaotic pion fields. As discussed in Refs. 25 and 26, when pions are produced mainly via resonance decay, the existence of resonances with different lifetimes ($\Gamma_\rho \sim 150$ MeV, $\Gamma_\omega \sim 10$ MeV) can significantly distort the shape of $R(q_o,q_t)$. For nuclear collisions, this last problem is not expected to be important though, as noted in Section II. Finally, the question of final state interactions has not been addressed. Often in applications,[7-12] there exist prescriptions such as dividing the $\pi^-\pi^-$ inclusive cross section by the $\pi^+\pi^-$ inclusive cross section to cancel the effects of final state interactions. However, not only Coulomb but also strong interactions differ for $\pi^-\pi^-$ and $\pi^+\pi^-$ pairs, and such prescriptions could therefore compound the distortions of $R(\tilde{k}_1,\tilde{k}_2)$ due to final state interactions.

To overcome the difficulties mentioned above, we turn in the next section to a more general method for calculating $R(\tilde{k}_1,\tilde{k}_2)$, based on a density matrix formalism for multiparticle production dynamics.

IV. COHERENT VERSUS CHAOTIC FIELDS

A. Density Matrix Formalism

At time $t = -\infty$, the initial state $|\phi_0\rangle$ is assumed to be specified. For nuclear collisions, $|\phi_0\rangle$ describes a state of two ground state nuclei and their relative motion. No pions are assumed to be present initially in $|\phi_0\rangle$. The asymptotic $t=+\infty$ final state $|\phi^+\rangle$ is then obtained formally by applying the *full* nuclear scattering S-matrix,

$$|\phi^+\rangle \equiv S|\phi_0\rangle \quad . \tag{4.1}$$

Note that $|\phi^+\rangle$ should not be confused with the Møller outgoing scattering wave. Needless to say, $|\phi^+\rangle$ is tremendously complicated and cannot be calculated since it requires the complete solution of the coupled pion – nuclear field equations. Nevertheless, we can attempt to parametrize $|\phi^+\rangle$ based on a physically plausible picture of the dynamics. The parameters specifying that picture would then be determined phenomenologically from inclusive cross sections. The hope in such a phenomenological approach is that the values of the parameters obtained will shed light on the dynamics of relativistic nuclear collisions.

However, before discussing specific parametrizations we proceed formally to calculate pion inclusive distributions from $|\phi^+\rangle$. The single (negative) pion inclusive distribution for momentum $\tilde{k}$ is given by

$$\begin{aligned} P_1(\tilde{k}) &\equiv \frac{1}{\sigma_\pi}\frac{d^3\sigma(\pi)}{d^3k} = \sum_X \left|\langle X|a(\tilde{k})|\phi^+\rangle\right|^2 \\ &= \langle\phi^+|a^+(\tilde{k})a(\tilde{k})|\phi^+\rangle = \langle\phi^+|N_\pi(\tilde{k})|\phi^+\rangle \\ &\equiv \mathrm{Tr}\{\rho^+ N_\pi(\tilde{k})\} \quad , \end{aligned} \tag{4.2}$$

where the sum over X and the trace are over a complete basis of nuclear and multipion configurations, $a^+(\tilde{k})$ and $N_\pi(\tilde{k})$ are the creation and number density operators for (negative) pions of momentum $\tilde{k}$, and

$$\rho^+ \equiv |\phi^+\rangle\langle\phi^+| \tag{4.3}$$

is the scattering density matrix with unit trace. Note that energy-momentum conservation is implicit in Eq. (4.2) because our definition of $|\phi^+\rangle$ includes an energy-momentum conserving δ-function via the S-matrix.[29] From Eq. (4.2) it is clear that the integral of $P_1(\tilde{k})$ over d^3k gives $\langle n_\pi\rangle$ as in Eq. (1.3), and that $P_1(\tilde{k})$ just counts the average number of pions in the final state with momentum $\tilde{k}$.

The double (negative) pion inclusive distribution is given in terms of ρ^+ by

$$\begin{aligned} P_2(\tilde{k}_1,\tilde{k}_2) &= \frac{1}{\sigma_\pi}\,\frac{d^6\sigma(\pi\pi)}{d^3k_1\, d^3k_2} \\ &= \sum_X |\langle X|a(\tilde{k}_2)a(\tilde{k}_1)|\phi^+\rangle|^2 \\ &= \mathrm{Tr}\left\{\rho^+\, a^+(\tilde{k}_1)a^+(\tilde{k}_2)a(\tilde{k}_2)a(\tilde{k}_1)\right\} . \end{aligned} \tag{4.4}$$

The integral of P_2 over $d^3k_1 d^3k_2$ then gives $\langle n_\pi(n_\pi-1)\rangle$ as in Eq. (1.2). Clearly, P_2 just counts the average number of (negative) pion pairs with momenta $\tilde{k}_1$ and $\tilde{k}_2$.

Equations (4.2) and (4.4) are written in terms of the density matrix ρ^+, because ρ^+ is simpler to parametrize than $|\phi^+\rangle$. In particular, we shall see that a very convenient way to parametrize ρ^+ is through an *ensemble average* over a given set of model states $|\phi_\alpha\rangle$ as

$$\rho^+ \approx \sum_\alpha p(\alpha)\, |\phi_\alpha\rangle\langle\phi_\alpha| \quad , \tag{4.5}$$

with $p(\alpha)$ being a (normalized) probability distribution for the parameters α specifying $|\phi_\alpha\rangle$. The $\approx$ sign in Eq. (4.5) means that we require ρ^+ together with Eqs. (4.2) and (4.4) to provide a good approximation to *only* single and double inclusive data. In other words, only those parametrizations that can reproduce the measured P_1 and P_2 shall be considered.

We note that the use of the density matrix formalism to compute inclusive distributions is well known in high energy physics (see for example Ref. 29). In the following subsections we utilize this formalism to analyze the difference between chaotic and coherent fields, as revealed through the correlation function $R(\tilde{k}_1,\tilde{k}_2)$.

B. Classical Current Parametrization

1. Coherent fields

In principle, we would like to solve the following field equation for the pion Heisenberg field $\phi(x)$:

$$(\Box + m_\pi^2)\phi(x) = J(x) \quad , \tag{4.6}$$

where $J(x)$ is the nuclear current operator acting as the source of pions. (Non-relativistically, $J = f_\pi \tilde{\nabla}\psi^\dagger\tilde{\sigma}\psi$.) What makes Eq. (4.6) intractable in general is that the field equations for the nuclear fields are coupled to the pion field also.

However, in a nuclear collision, our first expectation would be that multiple nucleon-nucleon collisions dominate the nuclear dynamics. As long as the number of produced pions is not large compared to the nucleon

number, we may expect that the pion source current $J(x)$ is not significantly altered by the presence of produced pions. Therefore our first approximation to the *nuclear* dynamics will be to ignore pion-nucleon rescattering. This approximation decouples the pion and nuclear field equations and replaces the pion source current operator in Eq. (4.6) by its expectation value. The current $J(x)$ then becomes a (c-number) space-time function. The resulting physical picture of the pion production dynamics is thus the same as that of bremsstrahlung radiation.[31] As the projectile nucleons collide with the target nucleons, pions are radiated due to the large decelerations involved.

We stress that Eq. (4.6) is still regarded as a field equation for $\phi(x)$, even though $J(x)$ is treated as a classical current source. This is in sharp contrast to the first quantized wave equation, Eq. (3.3), used in Ref. 3. As we shall see below, the importance of treating Eq. (4.6) as a field equation lies in the multipion nature of the final pion state.

Note also that the decoupling of the nuclear and pion field equations greatly simplifies the final density matrix ρ^+ in Eq. (4.3). In this approximation, ρ^+ factors into separate nuclear and pion density matrices, ρ_{nuc} and ρ_π, each with unit trace. We therefore only need to study ρ_π in order to compute $P_1(\tilde{k})$ and $P_2(\tilde{k}_1,\tilde{k}_2)$.

The solution of Eq. (4.6) and the construction of the S-matrix when J is treated as a classical current are discussed in detail in Ref. 31. See also Section Va. We only quote the main result: The final pion state $|\phi_\pi^+\rangle$ produced by a classical current source is a *coherent state* $|J\rangle$ given by[31]

$$|\phi_\pi^+\rangle = |J\rangle \equiv e^{-\bar{n}/2} \exp\left\{ i \int d^3k\, J(\tilde{k})\, a^+(\tilde{k}) \right\} |0\rangle \quad , \qquad (4.7)$$

where

$$J(\tilde{k}) \equiv \int d^4x \; \frac{e^{i\omega_k t - i\tilde{k}\cdot\tilde{x}}}{\sqrt{2\omega_k (2\pi)^3}} \; J(\tilde{x},t) \quad , \tag{4.8}$$

is the on-shell ($\omega_k = \sqrt{k^2 + m_\pi^2}$) Fourier transform of $J(\tilde{x},t)$, and

$$\bar{n} = \int d^3k \; |J(\tilde{k})|^2 \quad . \tag{4.9}$$

Observe that the state $|J\rangle$ is a special coherent superposition of pion states involving arbitrary numbers of pions. In terms of finite packet states, $|x_1 \ldots x_n\rangle_f$, localized at space-time points $x_1, \ldots x_n$ as defined in Appendix A, Eq. (A.1), we note that up to $(2\pi)^{3/2}$ in the definition of J,

$$\begin{aligned} |J\rangle &= e^{-\bar{n}/2} \; e^{i\phi_J^+(0)} |0\rangle \\ &= e^{-\bar{n}/2} \sum_{n=0}^{\infty} \frac{i^n}{n!} \; |x_1 = x_2 = \ldots = x_n = 0\rangle_J \quad . \end{aligned} \tag{4.10}$$

with $\phi_J^+(x)$ being the creation operator of a wavepacket centered at x as defined in Eq. (A.2). Thus an external classical current source $J(\tilde{x},t)$ produces an indefinite number of pions in wave packets with a space-time distribution $J(\tilde{x},t)$ centered at the origin. An additional property of $|J\rangle$ is that the multiplicity distribution for pions is a Poisson with a mean $\bar{n}$ given by Eq. (4.9). Therefore,

$$\langle n_\pi \rangle^2 = \langle n_\pi (n_\pi - 1) \rangle = \bar{n}^2 \quad . \tag{4.11}$$

The most useful property of $|J\rangle$ is that it is an eigenstate of the annihilation operators $a(\tilde{k})$, i.e.,

$$a(\tilde{k})|J\rangle = iJ(\tilde{k})\ |J\rangle \quad . \tag{4.12}$$

Therefore, removing one particle from the final state does *not* change the structure of the final state! Coherent states such as in Eq. (4.7) often arise in quantum optics and are used to characterize laser fields.[1]

The density matrix corresponding to this classical current model is

$$\rho_\pi \approx |J\rangle\langle J| \quad , \tag{4.13}$$

which describes a pure coherent state ($Tr\rho_\pi = Tr\rho_\pi^2 = 1$). We refer to Eq. (4.13) as the *coherent field* parametrization, the parameters here being those that specify $J(\tilde{k})$.

Utilizing Eq. (4.12), the m pion inclusive distribution is readily calculated, as in Ref. 29, to be

$$\begin{aligned} P_m(\tilde{k}_1, \ldots, \tilde{k}_m) &= Tr\left(\rho_\pi a^+(\tilde{k}_1) \ldots a^+(\tilde{k}_m) a(\tilde{k}_m) \ldots a(\tilde{k}_1)\right) \\ &= |J(\tilde{k}_1)|^2 \ldots |J(\tilde{k}_m)|^2 \quad . \end{aligned} \tag{4.14}$$

The two pion correlation function is therefore given by

$$R(\tilde{k}_1, \tilde{k}_2) = 1 \quad , \tag{4.15}$$

showing that pions radiated in a classical current model are *uncorrelated* in momentum space! In quantum optics,[1] the analog of Eq. (4.15) is the *absence* of intensity interference or the Hanbury-Brown and Twiss effect for laser fields. Similarly, there is no GGLP effect for coherent pions

even though BE symmetrization has automatically been taken into account in Eqs. (4.7) and (4.10).

We note finally that the multiplicity distribution of coherent pions which occupy a given momentum state $|\tilde{k}\rangle$ is also Poisson, with a mean $\langle n_\pi(\tilde{k})\rangle = |J(\tilde{k})|^2(2\pi)^3/V$, where V is the normalization volume.[31]

2. Charge-constrained coherent fields

One technical problem with coherent states involving charged bosons is that they are not eigenstates of charge. This problem can be easily bypassed, however, by considering the following charge-constrained generalization of the π^- coherent state[32]

$$|\phi^+(J,Z)\rangle \equiv \mathcal{N}^{\frac{1}{2}} \sum_{n=0}^{\infty} \frac{i^n}{n!} \int d^3k_1 \ldots d^3k_n \; J(\tilde{k}_1) \ldots J(\tilde{k}_n)$$

$$\times \; a^+(\tilde{k}_1) \ldots a^+(\tilde{k}_n) \; |0\rangle \otimes |\psi_n^+(Z)\rangle \quad , \tag{4.16}$$

where

$$\mathcal{N}^{-1} = \sum_{n=0}^{\infty} \frac{(\bar{n})^n}{n!} \langle \psi_n^+(Z) | \psi_n^+(Z) \rangle \quad , \tag{4.17}$$

and where $\bar{n}$ is given by Eq. (4.9), while $|\psi_n^+(Z)\rangle$ is a state containing no π^- but arbitrary multiple π^+ and π^o and nuclear configurations, constrained only to form an eigenstate of the total charge operator Q,

$$Q|\psi_n^+(Z)\rangle = (Z+n) \; |\psi_n^+(Z)\rangle \quad . \tag{4.18}$$

In Eq. (4.18), Z is the total charge of the initial (no pion) state $|\phi_o\rangle$ in Eq. (4.1). Equation (4.18) then also guarantees that $|\phi^+(J,Z)\rangle$ is an

eigenstate of charge with a total charge Z. With Eq. (4.16) we can now construct the combined pion-nuclear density matrix for a fixed charge Z as

$$\rho^{+} \approx |\phi^{+}(J,Z)\rangle \langle \phi^{+}(J,Z)| \quad , \tag{4.19}$$

from which we find

$$P_m(\tilde{k}_1 \ldots \tilde{k}_m) = |J(\tilde{k}_1)|^2 \ldots |J(\tilde{k}_m)|^2 \frac{\langle n_\pi(n_\pi-1)\ldots(n_\pi-m+1)\rangle}{\bar{n}^m} \quad , \tag{4.20}$$

where

$$\langle n_\pi(n_\pi-1)\ldots(n_\pi-m+1)\rangle = \bar{n}^m \left(\mathcal{n} \frac{\partial^m}{\partial \bar{n}^m} \mathcal{n}^{-1}\right) \quad , \tag{4.21}$$

is the m^{th} binomial moment of the negative pion multiplicity distribution.

The (negative) pion correlation function is therefore given by Eq. (4.15), just as for the simple coherent state parametrization, Eq. (4.13). Note, in fact, that if the states $|\psi_n^{+}(Z)\rangle$ were unit normalized, then $\mathcal{n}^{-1} = e^{\bar{n}}$, P(n) is Poisson, and hence Eq. (4.20) is identical to Eq. (4.14). In that case, Eq. (4.19) is completely equivalent to Eq. (4.13) as far as negative pion-inclusive cross sections are concerned. We therefore see that Eq. (4.15) is indeed possible for charged boson fields, and thus in the following sections we continue to use unconstrained coherent states.

Observe that the energy-momentum conservation has not been enforced in Eqs. (4.7) and (4.16). Since $J(\tilde{k})$ is to be constrained by the form of the single-pion inclusive distribution to vanish rapidly near kinematic boundaries, the inclusion of strict energy-momentum conservation for nuclear collisions would lead, in fact, to negligible corrections to Eq. (4.15).

C. Space-Time Picture and the Chaotic Field Limit

1. Classical current ensemble

In the previous section we showed that a single classical current produces a coherent pion field that exhibits no GGLP effect, even though BE statistics were properly taken into account. Since it is rather unlikely that the source current $J(x)$ is the same in every nuclear collision, we consider now a more general dynamical model that will enable us to incorporate variations of $J(x)$.

The physical picture we want to pursue is that of pions being produced in N separate nucleon-nucleon collisions in the spirit of intranuclear cascade models.[33] In this picture, the total pion source current $J(\tilde{x},t)$ would thus be a sum of N different currents, $J_i(\tilde{x},t)$,

$$J(x) = \sum_{i=1}^{N} J_i(x) \quad . \tag{4.22}$$

Each J_i is then taken to parametrize a different inelastic nucleon-nucleon collision. To incorporate also the space-time picture of the cascade model, we localize[16] the strength of each current around some "inelastic scattering center", $x_i = (\tilde{x}_i, t_i)$, as in Eq. (3.4).

If we parametrize the typical inelastic collision centered at $x = 0$ by $J_\pi(x)$, then the pion source current becomes

$$J(x) = \sum_{i=1}^{N} J_\pi(x - x_i) \quad . \tag{4.23}$$

The on-shell Fourier transform, Eq. (4.8), is given by

$$J(\tilde{k}) = J_\pi(\tilde{k}) \sum_{i=1}^{N} e^{i\omega_k t_i - i\tilde{k}\cdot\tilde{x}_i} \qquad (4.24)$$

where $\omega_k = \sqrt{k^2 + m^2}$. The space-time separation of the scattering centers therefore introduces a sum of phase factors in Eq. (4.24). In a given nuclear collision in which the x_i are fixed, the final pion state is again given by Eq. (4.7), but with J given by Eq. (4.24). Note that $|J\rangle$ is *not* equal to ψ_{12} of Eq. (3.5). It is also important to remark that at this stage we still have not incorporated final state interactions (see Section V). Our first aim is to study the effects of production dynamics on $R(\tilde{k}_1,\tilde{k}_2)$.

Since the number of inelastic scatterings, N, will vary from event to event as will the location of the space-time centers x_i $(i = 1, \ldots, N)$, we will have to average over the distribution, $P_S(N)$, of inelastic scatterings as well as the distributions, $\rho(x_i)$, of the centers x_i. An additional averaging over impact parameters will be discussed in section IV.C.3.

The distribution of N and x_i can be taken into account via an ensemble average with the pion sector density matrix given by

$$\rho_\pi \approx \sum_N P_S(N) \int d^4x_1\, \rho(x_1) \ldots d^4x_N\, \rho(x_N)\, |J\rangle\langle J| \quad . \qquad (4.25)$$

This pion density matrix then describes an ensemble of coherent final pion states. Note that the centers x_i are assumed to be uncorrelated in the spirit of independent multiple scattering models.

Using Eq. (4.14), the m-pion inclusive distribution in this model is given by

$$P_m(\tilde{k}_1, \ldots, \tilde{k}_m) = \sum_N P_S(N) \int d^4x_1\ \rho(x_1) \ldots d^4x_N \rho(x_N) \left\{ |J(\tilde{k}_1)|^2 \ldots |J(\tilde{k}_m)|^2 \right\}$$

$$\equiv \langle |J(\tilde{k}_1)|^2 \ldots |J(\tilde{k}_m)|^2 \rangle_{\{N, x_i\}} \quad . \tag{4.26}$$

It is clear from Eq. (4.26), that as a result of the ensemble average, there will now be non-trivial pion correlations in contrast to the pure coherent field result, Eq. (4.15).

For J given by Eq. (4.24), we then have

$$P_m(\tilde{k}_1, \ldots, \tilde{k}_m) = |J_\pi(\tilde{k}_1)|^2 \ldots |J_\pi(\tilde{k}_m)|^2\ \mathcal{F}_m(\tilde{k}_1, \ldots, \tilde{k}_m) \quad , \tag{4.27}$$

where the dynamical form factor $\mathcal{F}_m$ is given by

$$\mathcal{F}_m(\tilde{k}_1, \ldots, \tilde{k}_m) = \left\langle \left| \sum_{i=1}^{N} e^{ik_1 x_i} \right|^2 \ldots \left| \sum_{j=1}^{N} e^{ik_m x_j} \right|^2 \right\rangle_{\{N, x_k\}}$$

$$= \sum_{N=1}^{\infty} P_S(N) \left\{ \sum_{i_1=1}^{N} \cdots \sum_{i_{2m}=1}^{N} \right.$$

$$\left. \left\langle e^{ik_1 (x_{i_1} - x_{i_2})} \ldots e^{ik_m (x_{i_{2m-1}} - x_{i_{2m}})} \right\rangle_{\{x_i\}} \right\} \quad . \tag{4.28}$$

The evaluation of Eq. (4.28) is complicated only by the combinatorial problem of how many of the N^{2m} terms in the brackets have a given number of the indices $(i_1, \ldots, i_{2m})$ equal to one another. For a given index set we only need the relation

$$\langle e^{iqx_k} \rangle_{x_k} \equiv \int d^4x_k\ \rho(x_k)\ e^{iqx_k} = \rho(q) \quad , \tag{4.29}$$

where $\rho(q)$ is the Fourier transform of the scattering center distribution $\rho(x)$. Note that $\rho(\tilde{q}=0,\ q_o=0) = 1$ by unit normalization of $\rho(x)$.

For the case m=1, Eq. (4.28) is simply evaluated to be

$$\mathcal{J}_1(\tilde{k}) = \langle N \rangle + \langle N(N-1) \rangle \, |\rho(\tilde{k},\omega_k)|^2 \quad , \tag{4.30}$$

where $\langle N \rangle = \Sigma\ N\ P_S(N)$ is the average number of inelastic scatterings, and $\langle N(N-1) \rangle$ is the second binomial moment of $P_S(N)$. (For a Poisson distribution, as obtained in an intranuclear cascade model, $\langle N(N-1) \rangle = \langle N \rangle^2$.) The single pion inclusive distribution is thus

$$P_1(\tilde{k}) = |J_\pi(\tilde{k})|^2 \ \langle N \rangle \left\{ 1 + \frac{\langle N(N-1) \rangle}{\langle N \rangle} \, |\rho(\tilde{k},\omega_k)|^2 \right\} , \tag{4.31}$$

where $\omega_k \geq m_\pi$. Note that $P_1(\tilde{k})$ is *not* equal to the incoherent sum of the inclusive distributions, $|J_\pi(\tilde{k})|^2$, from each separate nucleon-nucleon collision. There is also an interference term growing as $\langle N^2 \rangle$ that depends on the pion wavelength, $|\tilde{k}|^{-1}$, and the nuclear dimension, R_o. For short wavelengths, $|\tilde{k}| >> R_o^{-1}$, $|\rho(k)|^2 << 1$, and Eq. (4.31) reduces to the incoherent case $P_1(\tilde{k}) \propto \langle N \rangle$. For long wavelengths, $|\tilde{k}| << R_o^{-1}$, so $|\rho(k)|^2 \approx |\rho(0,m_\pi)|^2$. Taking the $m_\pi \to 0$ limit for a moment and noting that $|\rho(0,0)|^2 = 1$, we see that the interference term then dominates and $P_1(\tilde{k}) \propto \langle N^2 \rangle$. This difference between the long and short wavelength limits for $m_\pi = 0$ is well known in the case of Thompson scattering of photons from atoms. Physically, it is due to the quantum property that a particle with a given wavelength $\lambda\!\!\!^{-}$ cannot resolve the structure of a system with dimensions less than $\lambda\!\!\!^{-}$. For a finite mass particle such as

the pion, there is an important difference however. The minimum frequency that a pion can have is $\omega(k=0) = m_\pi$. To see what effect this finite frequency has, consider a Gaussian parametrization[17] of the inelastic scattering center distribution:

$$\rho(\tilde{x},t) = \frac{(T R_x R_y R_z)^{-1}}{4\pi^2} \exp\left\{-\tfrac{1}{2}\left[(t/T)^2 + (x/R_x)^2 + (y/R_y)^2 + (z/R_z)^2\right]\right\}, \tag{4.32}$$

where T is the root mean square time duration, R_x is the root mean square x dimension, etc., of the space-time reaction volume containing the inelastic centers $(\tilde{x}_i,t_i)$. The Fourier transform is then simply

$$\rho(\tilde{k},\omega) = \exp\left\{-\tfrac{1}{2}\left[(\omega T)^2 + (k_x R_x)^2 + (k_y R_y)^2 + (k_z R_z)^2\right]\right\} . \tag{4.33}$$

With this parametrization we then have the following bound on $\rho(k)$,

$$|\rho(\tilde{k},\omega_k)|^2 \leq |\rho(0,m_\pi)|^2 = e^{-(m_\pi T)^2} . \tag{4.34}$$

As an estimate for the collision time T we note that in intranuclear cascade calculations,[33] pions are typically produced in nuclear collisions over a time interval $T \sim$ (5-10) fm/c. In that case $m_\pi T \gtrsim 5$ and $\exp(-(m_\pi T)^2) \ll 1$. Therefore, the collision time T is expected to be long compared to $m_\pi^{-1} \approx 1.4$ fm/c $\approx 5 \times 10^{-24}$ sec, and the interference term in Eq. (4.31) will be negligible even for $|\tilde{k}| = 0$. This is in sharp contrast to the zero mass case (Thomson scattering) where the interference term dominates in the $|\tilde{k}| = 0$ limit. If the interaction time were short, $T \lesssim m_\pi^{-1}$, then $\rho(0,m_\pi) \approx 1$, and the interference term would dominate for $|\tilde{k}| \lesssim 1/R_{x_i}$ even for the finite mass case. While we have considered

a specific model for $\rho(x)$ in Eq. (4.32), it is clear that also for the general case, the crucial factor that determines the importance of the interference term is the relative size of T and m_π^{-1}. As long as $T >> m_\pi^{-1}$,

$$P_1(\tilde{k}) \approx |J_\pi(\tilde{k})|^2 \langle N \rangle \quad , \tag{4.35}$$

with small corrections depending on the specific form of ρ.

We note that the smallness of the interference term can be tested experimentally by measuring the $A^{\alpha(k)}$ dependence of the pion-inclusive cross section on the number of incident nucleons A. For equal mass projectile-target combinations $\alpha(k) \approx 1.67$ if pions are produced incoherently while $\alpha(k) \approx 2.67$ if the interference term dominates. (These estimates are based on the assumption that the total pion cross section goes as $A^{2/3}$ while the number of inelastic scatterings $\langle N \rangle \propto A^1$.) Another consequence of Eq. (4.35) is that the average (negative) pion multiplicity is well approximated by

$$\langle n_\pi \rangle \approx \bar{n}_\pi \langle N \rangle \quad , \tag{4.36}$$

where

$$\bar{n}_\pi = \int d^3k \; |J_\pi(\tilde{k})|^2 \tag{4.37}$$

is the average (negative) pion multiplicity from each inelastic nucleon-nucleon collision. In the 1 GeV range, $\bar{n}_\pi \approx 0.7$, and thus the average number of inelastic collisions, $\langle N \rangle$, is roughly given by $\langle n_\pi \rangle$. (Note that the total number of binary collisions may be much larger than $\langle N \rangle$.) The smallness of the interference term in

Eq. (4.31) would thus result in an A^1 dependence of $\langle n_\pi \rangle$. Evidence for an A^2 dependence of $\langle n_\pi \rangle$ would, in contrast, indicate the importance of the interference term and reflect an unexpectedly short interaction time in this cascade picture.

We note finally that the small correction term in Eq. (4.35) also decreases very rapidly with increasing $|\tilde{k}|$. For $|\tilde{k}| \gtrsim m_\pi$, $|\rho(\tilde{k},\omega_k)|^2 \ll 1$ regardless of the value of T since the nuclear dimensions are large compared to m_π^{-1} ($R_{x_i} \approx 3m_\pi^{-1}$). We conclude that as long as pions are produced by separate inelastic collisions over a long enough time or we consider $|\tilde{k}| \gtrsim m_\pi$, the single inclusive distribution is well approximated by the incoherent sum of the distributions from each collision.

Consider now the double pion inclusive distribution. From Eqs. (4.27) and (4.28) we need to calculate $\mathcal{F}_2(\tilde{k}_1,\tilde{k}_2)$. There are now N^4 terms in the bracket, but most of the terms give rise to the same contribution. For example, there are $N(N-1)(N-2)(N-3)$ terms such that all four indices $(i_1,\ldots,i_4)$ are distinct. Noting Eq. (4.29), the ensemble average of each of these terms is simply $|\rho(k_1)|^2|\rho(k_2)|^2$. Similarly there are $N(N-1)$ terms such that $i_1=i_4$, $i_2=i_3$, but $i_1\neq i_2$. Each of these terms gives rise to $|\rho(k_1-k_2)|^2$. Collecting all terms, we find

$$\begin{aligned}\mathcal{F}_2(\tilde{k}_1,\tilde{k}_2) &= \langle N^2\rangle + \langle N(N-1)\rangle\{|\rho(k_1-k_2)|^2 + |\rho(k_1+k_2)|^2\} \\ &+ \langle N^2(N-1)\rangle\{|\rho(k_1)|^2 + |\rho(k_2)|^2\} \\ &+ \langle N(N-1)(N-2)\rangle 2\mathrm{Re}\{\rho(k_1-k_2)\rho^*(k_1)\rho(k_2) + \rho(k_1+k_2)\rho^*(k_1)\rho^*(k_2)\} \\ &+ \langle N(N-1)(N-2)(N-3)\rangle |\rho(k_1)|^2 |\rho(k_2)|^2 \quad . \qquad (4.38)\end{aligned}$$

First note that if N=1, i.e., there is only one current source, then $\mathcal{F}_2 \equiv 1$, and we recover the coherent field result, Eq. (4.14).

As the number of sources N increases, more of the terms in Eq. (4.38) start contributing. The various terms arise from the interference between different possible amplitudes for producing two pions. In order to have a clearer understanding of Eq. (4.38), it is instructive to identify the amplitudes that lead to the various terms.

In this classical current model there are two ways in which a pion pair can be created. Either the two pions are produced by two different sources ($x_i \neq x_j$) or they are produced by the same source. Denote the amplitude to produce the two pions from different sources i and j, $i \neq j$, by A_{ij}. Denote the amplitude to produce the two pions by the same source i by B_i. The total amplitude to produce the two pions is then

$$M = \sum_{i>j} \{A_{ij} + A_{ji}\} + \sum_i B_i \quad , \tag{4.39}$$

as illustrated in Fig. 1. The probability of observing the two pions is then $|M|^2$. By grouping the N^4 terms in $|M|^2$, we can associate the following interference terms with each of the terms in Eq. (4.38):

$$\sum_{i\neq j} |A_{ij}|^2 + \sum_i |B_i|^2 \longleftrightarrow \langle N^2 \rangle \tag{4.40a}$$

$$\sum_{i\neq j} A_{ij} A^*_{ji} \longleftrightarrow \langle N(N-1) \rangle \, |\rho(k_1 - k_2)|^2 \quad , \tag{4.40b}$$

$$\sum_{i\neq j} B_i B^*_j \longleftrightarrow \langle N(N-1) \rangle \, |\rho(k_1 + k_2)|^2 \quad , \tag{4.40c}$$

$$\left\{ \sum_{i\neq j\neq k} (A_{ij}A^*_{ik} + A_{ji}A^*_{ki}) \longleftrightarrow \langle N^2(N-1) \rangle \{ |\rho(k_1)|^2 + |\rho(k_2)|^2 \} \right.$$

$$\left. + \sum_{i\neq j} (A_{ij}B^*_j + A_{ji}B^*_j + \text{c.c.}) \right\} \quad , \tag{4.40d}$$

$$\sum_{i\neq j\neq k} (A_{ij}B^*_k + \text{c.c.}) \longleftrightarrow \langle N(N-1)(N-2) \rangle \times 2\text{Re}(\rho(k_1+k_2)\rho^*(k_1)\rho^*(k_2)) \quad , \tag{4.40e}$$

$$\sum_{i\neq j\neq k} (A_{ij}A^*_{jk} + A_{ji}A^*_{kj}) \longleftrightarrow \langle N(N-1)(N-2) \rangle \times 2\text{Re}(\rho(k_1-k_2)\rho^*(k_1)\rho(k_2)) \quad , \tag{4.40f}$$

$$\sum_{i\neq j\neq k\neq \ell} A_{ij}A^*_{k\ell} \longleftrightarrow \langle N(N-1)(N-2)(N-3) \rangle \, |\rho(k_1)|^2 |\rho(k_2)|^2 \quad . \tag{4.40g}$$

These equations display the physical origin of each of the terms in Eq. (4.38). Note especially the origin of $|\rho(k_1-k_2)|^2$ from Eq. (4.40b). It is due to the interference between the amplitude, $A_{ij}(k_1,k_2) \propto e^{ik_1x_i} e^{ik_2x_j}$ for producing a pion with momentum k_1 from source i together with a pion with momentum k_2 from source $j\neq i$ and the amplitude $A_{ji}(k_1,k_2)$ for producing a pion with momentum k_2 from source i together with a pion with momentum k_1 from source $j\neq i$. This is clearly the Bose-Einstein statistics interference term as considered in Section III. However, in contrast to the results of Section III, there also appear many more interference terms due to the multiparticle dynamics. The term in Eq. (4.40c), for example, arises only because a given source can emit two or more pions by itself.

What Eq. (4.38) demonstrates in this simple analytical model is that the details of the multiparticle production dynamics can lead to major modifications of the ideal Bose-Einstein correlation result, Eq. (3.6).

In the case of nuclear collisions though, we can argue that the correction terms in Eqs. (4.40c-g) are very small. This follows again from the fact that the collision time T is long compared to m_π^{-1}. Thus Eq. (4.34) implies that all terms containing $\rho(k_1)$ and $\rho(k_2)$ are negligible. Noting that $|\rho(k_1+k_2)|^2 = |\rho(\tilde{k}_1+\tilde{k}_2,\ \omega_1+\omega_2)|^2 \leq |\rho(0,2m_\pi)|^2$, the term from Eq. (4.40c), is then also negligible. For nuclear collisions we can therefore well approximate $\mathcal{J}_2(\tilde{k}_1,\tilde{k}_2)$ by

$$\mathcal{J}_2(\tilde{k}_1,\tilde{k}_2) = \{\langle N^2\rangle + \langle N(N-1)\rangle\ |\rho(k_1-k_2)|^2\}\ \{1+\varepsilon\} \qquad (4.41)$$

with

$$\varepsilon \sim O(\langle N\rangle|\rho(0,m_\pi)|^2) \ll 1 \quad .$$

Note that $\rho(k_1-k_2) = \rho(\tilde{k}_1-\tilde{k}_2,\omega_1-\omega_2)$ can be of order unity since for $|\tilde{k}_1| = |\tilde{k}_2|$, $\omega_1-\omega_2 = 0$, and $\rho(0,0) = 1$. The only interference term that survives for long interaction times is that due to Bose-Einstein symmetrization, Eq. (4.40b).

From Eq. (4.41), we calculate next the second binomial moment of the multiplicity distribution. Noting Eq. (4.36), we find

$$\langle n_\pi(n_\pi - 1)\rangle = \langle n_\pi\rangle^2 \frac{\langle N^2\rangle}{\langle N\rangle^2}(1+\varepsilon+\delta) \tag{4.42}$$

where

$$\varepsilon \sim O(\langle N\rangle |\rho(0,m_\pi)|^2)$$

and

$$\delta = \frac{\langle N(N-1)\rangle}{\langle N^2\rangle \bar{n}_\pi^2}\int d^3k_1 d^3k_2 |J_\pi(\tilde{k}_1)\rho(k_1-k_2)J_\pi(\tilde{k}_2)|^2$$

$$\sim O(1/A) \tag{4.43}$$

where A is the number of nucleons involved in the nuclear collision. To arrive at this estimate for δ in Eq. (4.43) we used $\langle N(N-1)\rangle/\langle N^2\rangle \leq 1$ and estimated the integral divided by $\bar{n}_\pi^2$ to be $O((\langle k_\pi\rangle R_o)^{-3})$ via Eq. (A.21) in Section A.2 of Appendix A. Here, $\langle k_\pi\rangle$ is the average cm pion momentum produced by $J_\pi(k)$ and R_o is the average radius of $\rho(x,t)$. Since $(\langle k_\pi\rangle R_o)^3 \sim O(A)$ for relativistic nuclear collisions as we show in Appendix A, we finally get Eq. (4.43).

We note that for one source current, $P_S(N) = \delta_{N,1}$, $\varepsilon = \delta = 0$ rigorously, as expected because pions are Poisson distributed in a coherent state, Eq. (4.11). As the number of sources increases, $\varepsilon > 0$ and $\delta > 0$ lead to non-Poisson behavior. However, as the number of sources becomes very large, $\delta \to 0$, and as long as the total interaction time grows

with $\langle N \rangle$ such that

$$\langle N \rangle \rho |(0,m_\pi)|^2 \ll 1 \tag{4.44}$$

is satisfied, the Poisson relation between the first two moments is recovered again.

2. The chaotic field limit

From the results of the last section on the classical current ensemble, we can now derive a set of conditions under which the correlation function $R(\tilde{k}_1,\tilde{k}_2)$ reduces to the ideal BE form of Eq. (3.6). In terms of the form factors $\mathcal{F}_m$,

$$R(\tilde{k}_1,\tilde{k}_2) = \frac{\mathcal{F}_2(\tilde{k}_1,\tilde{k}_2)}{\mathcal{F}_1(\tilde{k}_1)\mathcal{F}_1(\tilde{k}_2)} \frac{\langle n_\pi \rangle^2}{\langle n_\pi(n_\pi-1)\rangle} . \tag{4.45}$$

In general, we see from (4.31) and (4.38) that R is much more complicated than Eq. (3.6) due to interference of multipion production amplitudes. However, for long interaction times, for which Eq. (4.44) is satisfied, R reduces to

$$R(\tilde{k}_1,\tilde{k}_2) = 1 + \left(1 - \frac{\langle N \rangle}{\langle N^2 \rangle}\right) |\rho(k_1-k_2)|^2 , \tag{4.46}$$

with corrections $O(1/A)$ from Eq. (4.43). In the limit $\langle N \rangle \gg 1$, Eq. (4.46) therefore reduces to the ideal BE result, Eq. (3.6).

We saw that the long time constraint, Eq. (4.44), leads to Eq. (4.35). Now we see that Eq. (3.6) follows from Eq. (4.45) in the limit when a large number of sources produce pions incoherently with respect to each other in a large space time volume. This type of pion field ensemble is thus referred to as a chaotic field.

We have thus found one dynamical model that leads to the ideal BE form, Eq. (3.6), in the appropriate limit.[16,34] To demonstrate that the essential ingredient leading to this result is the space-time picture of the distribution of sources and not the specific dynamical model involving classical currents, we present another derivation of Eq. (3.6) in Appendix A. That derivation deals exclusively with a space-time parametrization of ρ_π, Eqs. (A.6), using normalized wave packets localized in space-time. Again Eq. (3.6) follows in the limit, Eq. (A.15), where the average spacing between two localized packets is much larger than the dimensions of the packets. In that case the relative phases between any two pions, $\Delta\phi \approx k_1 x_1 - k_2 x_2$, is essentially randomly distributed between 0 and 2π, and the resulting pion field is again chaotic.

We note that there is a mathematical short-cut to obtaining Eq. (4.46) when condition (4.44) is satisfied. That is to introduce random phases ϕ_i between the currents $J_i(x)$ in Eq. (4.22). The Fourier transform of the chaotic source current in this space-time picture is thus defined as

$$J_{ch}(\tilde{k}) = J_\pi(\tilde{k}) \sum_{i=1}^{N} e^{i\phi_i} e^{i\omega_k t_i - i\tilde{k}\cdot\tilde{x}_i} \tag{4.47}$$

The m-pion inclusive distribution is then calculated as in Eq. (4.26) except that we must also average over all ϕ_i from 0 to 2π. The resulting form factors then lead directly to Eqs. (4.35, 4.41, 4.46). The additional interference terms in Eqs. (4.31, 4.38) vanish upon averaging over ϕ_i. We shall use this mathematical short-cut to chaotic fields below and in Section IV.D.

An important property of the chaotic field limit is that the multiplicity distribution of pions which occupy a given momentum state $|\tilde{k}\rangle$, denoted by $P(n;\tilde{k})$, becomes a Bose-Einstein (geometric) distribution.[1] To see this, we recall from Section IV.B.1 that for a coherent state $|J\rangle$, $P(n;\tilde{k})$ is a Poisson distribution with mean $|J(\tilde{k})|^2/\Omega$, where $(2\pi)^3\Omega$ is the normalization volume arising in the usual transition from discrete sums to integrals ($\Sigma_i \to \Omega \int d^3k$). For a chaotic ensemble of coherent states, similar to Eq. (4.25), we thus have

$$P(n;\tilde{k}) = \lim_{\langle N\rangle \to \infty} \left\langle \frac{(|J_{ch}(\tilde{k})|^2/\Omega)^n}{n!} \exp[-|J_{ch}(\tilde{k})|^2/\Omega] \right\rangle_{\{N,\phi_i,x_i\}} \tag{4.48}$$

where $J_{ch}(\tilde{k})$ is given by Eq. (4.47) -- the ensemble average over the ϕ_i is just a short-cut to incorporating condition (4.44). As a device for taking the limit $\langle N\rangle \to \infty$, it is convenient to use a sequence of "spike" source number distributions, $P_S(N') = \delta_{N'N}$, with $N \to \infty$. This, plus the definition (4.47) and the (now exact) result (4.35), allows us to express the chaotic current strength in the form

$$|J_{ch}(\tilde{k})|^2 = \lim_{N\to\infty} \frac{P_1(\tilde{k})}{N} \left| \sum_{i=1}^{N} e^{i\phi_i} e^{ikx_i} \right|^2 , \tag{4.49}$$

where $P_1(\tilde{k})$ is the single pion-inclusive distribution, which we shall hold fixed as $N \to \infty$. To evaluate Eq. (4.48), it is sufficient to obtain the probability density for the limiting random variable $|J_{ch}(\tilde{k})|^2$ to have the value $|J|^2$. In Appendix B we show this to be

$$P_{ch}(|J|^2;\tilde{k}) = (P_1(\tilde{k}))^{-1} \exp\{-|J|^2/P_1(\tilde{k})\} \quad . \tag{4.50}$$

Therefore,

$$P(n;\tilde{k}) = \int_0^\infty d|J|^2 \; P_{ch}(|J|^2;\tilde{k}) \; \frac{(|J|^2/\Omega)^n}{n!} \exp[-|J|^2/\Omega]$$

$$= \frac{(P_1(\tilde{k})/\Omega)^n}{(1 + P_1(\tilde{k})/\Omega)^{n+1}} \tag{4.51}$$

which is the Bose-Einstein (geometric) distribution with mean $P_1(\tilde{k})/\Omega$. We note[24] that the thermodynamic (fireball) pion multiplicity distribution for momentum state $|\tilde{k}\rangle$ is a special case of the chaotic field result, Eq. (4.51), when the single pion-inclusive distribution is thermal,[1] i.e., when

$$P_1(\tilde{k}) = \Omega(e^{\beta\omega_k} - 1)^{-1} \quad , \tag{4.52}$$

where β is the inverse temperature and $(2\pi)^3\Omega$ is the volume of the system.

3. Impact parameter average

Up to now we have implicitly considered a nuclear collision at a fixed impact parameter for which $\rho(\tilde{x},t)$ could be calculated, for example, via an intranuclear cascade model.[33] The reaction volume specified by ρ clearly depends[30] on the impact parameter, $\tilde{b}$. Obviously that volume is largest for central collisions, $b \approx 0$, and smallest for peripheral collisions, $b \approx R_{A_1} + R_{A_2}$. Likewise, the distribution of inelastic scatterings, $P_S(N)$ in Eq. (4.25) must also depend on b.

It is possible to select experimentally a range of impact parameters, specified by a distribution $B(\tilde{b})$, by an appropriate trigger system based, for example, on associated multiplicities or azimuthal symmetry or asymmetry of reaction products. In Ref. 19, for example, the inelastic trigger mode for Ar +Pb corresponds to $B(\tilde{b}) = \theta(b_{max} - b)/2\pi b_{max}^2$, with $b_{max} = 9.6$ fm, as determined in Ref. 24.

The impact parameter distribution can be incorporated into ρ_π as

$$\rho_\pi \approx \int d^2b\ B(\tilde{b}) \sum_N P_S(N,\tilde{b}) \int d^4x_1 \ldots d^4x_N\ \rho(x_1,\tilde{b}) \ldots \rho(x_N,\tilde{b})\ |J\rangle\langle J| \quad , \tag{4.53}$$

which is the obvious generalization of Eq. (4.25). The m-pion inclusive distribution in Eq. (4.26) will thus involve an additional $\int d^2b\ B(\tilde{b})$

integration, and $\mathcal{F}_m$ in Eqs. (4.27) and (4.28) also acquires this impact parameter average. Since Eq. (4.44) is expected to hold for all but the most peripheral collisions, which are excluded anyway in inelastic triggered data, we then have from Eqs. (4.35) and (4.41):

$$P_1(\tilde{k}) \approx |J_\pi(\tilde{k})|^2 \langle N \rangle_B \quad , \tag{4.54}$$

and

$$P_2(\tilde{k}_1,\tilde{k}_2) \approx |J_\pi(\tilde{k}_1)|^2 |J_\pi(\tilde{k}_2)|^2 \{\langle N^2 \rangle_B + \langle N(N-1)\,|\rho(k_1-k_2)|^2 \rangle_B\} \, , \tag{4.55}$$

where $\langle \ldots \rangle_B$ denotes the impact parameter average for a particular experimental trigger system specified by $B(\tilde{b})$.

In the chaotic field limit where $\langle N(\tilde{b}) \rangle >> 1$ for all $\tilde{b}$ in $B(\tilde{b})$, the correlation function therefore reduces to

$$R(\tilde{k}_1,\tilde{k}_2) \approx 1 + \langle |\rho(k_1 - k_2)|^2 \rangle_B \quad . \tag{4.56}$$

To get the maximum geometrical information out of R it is clearly necessary to select as narrow a range of $\tilde{b}$ with $B(\tilde{b})$ as experimentally possible, for R measures the impact-parameter-averaged space-time reaction volume in the chaotic field limit.

D. Partially Coherent Pion Fields

1. Definition of degree of coherence

If the pion production dynamics in nuclear collisions were simply a superposition of isolated $n + n \to \pi + X$ as in intranuclear cascade models, then the results of Section IV.C and Appendix A suggest that the pion correlation function is dominated by BE interference. On the other hand,

speculations have arisen[16,28] suggesting that collective instabilities involving the pion field could occur in dense nuclear systems. In that case, it is possible that in addition to the chaotic field component coming from isolated nucleon-nucleon collisions, there may be a coherent field component resulting from the collective action of a large group of nucleons.

To study the effect of such a possible coherent and chaotic field admixture on the correlation function, consider the following model of the pion source:

$$J(\tilde{k}) = J_o(\tilde{k}) + J_{ch}(\tilde{k}) \quad , \tag{4.57}$$

where J_o describes the current due to the collective action of a group of nucleons, while J_{ch} is the current describing the chaotic component due to isolated nucleon-nucleon collisions given by Eq. (4.47).

The average number of pions in the chaotic component is then

$$n_{ch} = \int d^3k \, \langle |J_{ch}(\tilde{k})|^2 \rangle_{\{N,\phi_i,x_i\}} = \langle N \rangle \bar{n}_\pi \quad , \tag{4.58}$$

with $\bar{n}_\pi$ given by Eq. (4.37).

On the other hand, the average number of pions in the coherent component is

$$n_o = \int d^3k \, |J_o(\tilde{k})|^2 \quad . \tag{4.59}$$

The single pion inclusive distribution is then found to be

$$\begin{aligned} P_1(\tilde{k}) &= \langle n_\pi(\tilde{k}) \rangle = \langle |J_o(\tilde{k}) + J_{ch}(\tilde{k})|^2 \rangle_{\{N,\phi_i,x_i\}} \\ &= |J_o(\tilde{k})|^2 + \langle N \rangle |J_\pi(\tilde{k})|^2 \\ &\equiv n_o(\tilde{k}) + n_{ch}(\tilde{k}) \quad , \end{aligned} \tag{4.60}$$

from which the total average pion multiplicity is seen to be $\langle n_\pi \rangle = n_o + n_{ch}$. In Eq. (4.60), $n_o(\tilde{k})$ and $n_{ch}(\tilde{k})$ are the average number densities of coherent and chaotic field pions with momentum $\tilde{k}$.

The double pion inclusive distribution is in turn given by

$$\begin{aligned} P_2(\tilde{k}_1,\tilde{k}_2) &= \langle |J_o(\tilde{k}_1) + J_{ch}(\tilde{k}_1)|^2 |J_o(\tilde{k}_2) + J_{ch}(\tilde{k}_2)|^2 \rangle_{\{N,\phi_i,x_i\}} \\ &= |J_o(\tilde{k}_1)|^2 |J_o(\tilde{k}_2)|^2 \\ &+ \langle N \rangle [|J_o(\tilde{k}_1)|^2 |J_\pi(\tilde{k}_2)|^2 + |J_o(\tilde{k}_2)|^2 |J_\pi(\tilde{k}_1)|^2] \\ &+ |J_\pi(\tilde{k}_1)|^2 |J_\pi(\tilde{k}_2)|^2 \{\langle N^2 \rangle + \langle N(N-1) \rangle |\rho(k_1-k_2)|^2\} \\ &+ 2\mathrm{Re}\left\{(J_o^*(\tilde{k}_1)J_o(\tilde{k}_2))(J_\pi^*(\tilde{k}_2)J_\pi(\tilde{k}_1)) \langle N \rangle \rho(k_1-k_2)\right\}. \end{aligned} \tag{4.61}$$

The second binomial moment is then

$$\langle n_\pi(n_\pi - 1) \rangle = (n_o + n_{ch})^2 + n_{ch}^2 \varepsilon + n_o n_{ch} \delta \quad , \tag{4.62}$$

where $\varepsilon, \delta \sim O(1/A)$, by estimates of integrals as in Appendix A.2.

The correlation function is thus finally given by

$$\begin{aligned} R(\tilde{k}_1,\tilde{k}_2) &= 1 + \frac{n_{ch}(k_1)}{P_1(k_1)} \frac{n_{ch}(k_2)}{P_1(k_2)} |\rho(k_1-k_2)|^2 \\ &+ 2\mathrm{Re}\left\{\frac{(J_o^*(k_1)J_\pi(k_1))}{P_1(k_1)} \frac{(J_\pi^*(k_2)J_o(k_2))}{P_1(k_2)} \langle N \rangle \rho(k_1-k_2)\right\} \end{aligned} \tag{4.63}$$

with corrections $O(1/A)$. Note especially the value of R at the intercept $\tilde{k}_1 = \tilde{k}_2 = \tilde{k}$.

$$R(\tilde{k},\tilde{k}) = 2 - (D(\tilde{k}))^2 \quad , \tag{4.64}$$

where we have defined the degree of coherence of mode $\tilde{k}$ as

$$D(\tilde{k}) = \frac{|J_o(\tilde{k})|^2}{P_1(\tilde{k})} = \frac{n_o(\tilde{k})}{n_o(\tilde{k}) + n_{ch}(\tilde{k})} \quad . \qquad (4.65)$$

Note that with this definition of the degree of coherence for mode $\tilde{k}$, $D(\tilde{k})$ is simply the fraction of pions with momentum $\tilde{k}$ produced by the coherent source J_o.

If we further assume that $J_o(k)$, $J_\pi(k)$, and $\rho(k)$ are real (as for a Gaussian parametrization, e.g., Eq. (4.33)), then we can write

$$R(\tilde{k}_1,\tilde{k}_2) = 1 + (1-D(\tilde{k}_1))(1-D(\tilde{k}_2))\,\rho^2(k_1-k_2) + 2[D(\tilde{k}_1)D(\tilde{k}_2)(1-D(\tilde{k}_1))(1-D(\tilde{k}_2))]^{\frac{1}{2}}\,\rho(k_1-k_2) \quad . \qquad (4.66)$$

In the chaotic field limit, $D(\tilde{k}) = 0$ and Eq. (4.66) reduces to the ideal BE interference result, Eqs. (3.6) and (4.46). In the opposite limit of a pure coherent field, $D(\tilde{k}) = 1$, and Eq. (4.66) reduces to Eq. (4.15). For a partially coherent field with $0 < D(\tilde{k}) < 1$, and $D(\tilde{k})$ varying from mode to mode, $R(\tilde{k}_1,\tilde{k}_2)$ has the more complex structure of Eq. (4.66).

Equation (4.66) is our main result of Section IV, showing that R contains both geometrical and dynamical information. As is clear from the way that the functional form of $D(\tilde{k})$ and $\rho(k_1-k_2)$ enter Eq. (4.66), for partially coherent fields we cannot simply extract $\rho(q)$ from $R(\tilde{k}_1,\tilde{k}_2)$ without first determining $D(\tilde{k})$ via Eq. (4.64).

To illustrate the effect of a finite degree of coherence, $D \neq 0$, on the apparent radius of the system, consider a spherical source with root mean square radius R_o. To determine R_o from correlation data, $R(\tilde{k}_1,\tilde{k}_2)$,

the usual procedure is to fit $R(\tilde{k}_1,\tilde{k}_2)$ with a simple parametrization such as in Eq. (3.7) or its Gaussian analog. To eliminate the dependence of the shape of $R(\tilde{k}_1,\tilde{k}_2)$ on the interaction time, the difference $\tilde{q} = \tilde{k}_1-\tilde{k}_2$ must be varied so that $q_o = \omega_1-\omega_2 = 0$ is held fixed. In other words, we consider only <u>equal</u> energy pions ($|\tilde{k}_1| = |\tilde{k}_2|$) and vary the angle between $\tilde{k}_1$ and $\tilde{k}_2$. Letting $\tilde{K} = \frac{1}{2}(\tilde{k}_1+\tilde{k}_2)$ be the average pion momentum, an effective radius R_{eff} could be obtained by fitting $R(\tilde{k}_1,\tilde{k}_2)$ with the two parameter form[12]

$$R(\tilde{K}+\tilde{q}/2;\ \tilde{K}-\tilde{q}/2)\Big|_{\tilde{K}\cdot\tilde{q}=0} \approx 1 + \lambda\exp[-q^2R_{eff}^2] \quad . \tag{4.67}$$

In Ref. 12, λ was interpreted as the interfering fraction of all $\pi^-\pi^-$ pairs and R_{eff} was interpreted as the chaotic source radius. From Eq. (4.64) we would interpret λ as $1-(D(\tilde{K}))^2$. In practice λ and R_{eff} can be determined by a least squares fit to the data. For our purposes we define R_{eff} through

$$R_{eff}^2 = -\tfrac{1}{2}\lim_{q\to 0}\frac{\partial^2}{\partial q^2}\frac{R(\tilde{K}+\tilde{q}/2,\ \tilde{K}-\tilde{q}/2)}{(R(\tilde{K},\tilde{K})-1)}\Big|_{\tilde{K}\cdot\tilde{q}=0} \quad . \tag{4.68}$$

Note that the constraint $\tilde{K}\cdot\tilde{q}=0$ insures that both pions have the same energy. If the chaotic source distribution is given by $|\rho(\tilde{q},q_o=0)|^2 = \exp[-q^2R_o^2]$ and the variation of $D(\tilde{K}\pm\tilde{q}/2)$ with respect to q is small compared to R_o; i.e., $|\nabla D(\tilde{K})| \ll R_o$, then from Eqs. (4.66) and (4.68) we get

$$R_{eff}^2 \approx R_o^2/(1+D(\tilde{K})) \tag{4.69}$$

with corrections $O(|\nabla D|^2,\nabla^2 D)$. Equation (4.69) shows that the effective radius is smaller than the true radius for partially coherent fields. Furthermore, R_{eff} may then have an explicit dependence on the mean pion momentum vector, $\tilde{K}$. It is therefore clear that for partially coherent fields, $D(\tilde{k})$ must first be determined before geometrical information about

the reaction volume can be obtained from $R(\tilde{k}_1,\tilde{k}_2)$.

In addition, once $D(\tilde{k})$ is known, then the total number of pions in the coherent and chaotic components can be determined from

$$n_o = \int d^3k\ D(\tilde{k})\ P_1(\tilde{k}) \tag{4.70}$$

and

$$n_{ch} = \int d^3k\ (1 - D(\tilde{k}))P_1(\tilde{k}) \quad . \tag{4.71}$$

Note that while it is possible to define a global degree of coherence via $n_o/(n_o+n_{ch})$ as in Ref. 13, it is clear that the degree of coherence per mode $D(\tilde{k})$ is a much more complete way of characterizing partially coherent fields.

To summarize these results, we illustrate in Fig. 2 the expected form of the correlation function for partially coherent fields. We consider a case where $D(\tilde{k})$ is slowly varying so that Eq. (4.69) holds.

2. Effect of impact parameter average

As in Eq. (4.53), we can incorporate an impact parameter average over a range of impact parameters specified by a distribution $B(\tilde{b})$. In addition to the $\tilde{b}$ dependence of the chaotic field component, we may also expect that if there is a coherent field component, then the source $J_o(\tilde{k};\tilde{b})$ may depend sensitively on $\tilde{b}$. In particular, $n_o(\tilde{b})$ is expected to be greatest for central collisions which involve the largest number of nucleons in the interaction region and, thus, maximize the probability of collective phenomena.

The effect of such an impact parameter average is to introduce $\int d^2b\ B(\tilde{b})$ on the right-hand side of both Eqs. (4.60) and (4.61). Because an average over a product of functions can be quite different from the

product of their averages, the resulting correlation function for an arbitrary B(b) will not have the simple structure of Eq. (4.66).

In order to extract information out of $R(\tilde{k}_1,\tilde{k}_2)$ it is absolutely vital to select a sufficiently narrow band of impact parameters, Δb, via $B(\tilde{b})$ over which the degree of coherence $D(\tilde{k};\tilde{b})$ satisfies $|\partial D/\partial b| \ll D(\tilde{k};\tilde{b})/|\Delta b|$. We must therefore insure that

$$\frac{|J_o(\tilde{k},\tilde{b})|^2}{|J_o(\tilde{k},\tilde{b})|^2 + \langle N(\tilde{b})\rangle |J_\pi(\tilde{k})|^2} \approx D_B(\tilde{k}) \equiv \langle D(\tilde{k};\tilde{b})\rangle_B \qquad (4.72)$$

is approximately independent of b over the range Δb specified by $B(\tilde{b})$. Note that Eq. (4.72) does not prevent $J_o(\tilde{k},\tilde{b})$ and $J_{ch}(\tilde{k},\tilde{b})$ from varying with $\tilde{b}$ over that range. It only requires that the ratio of the number of coherent to chaotic field pions in each mode $\tilde{k}$ be independent of $\tilde{b}$ over a limited range. In effect, all the variation of P_1 and P_2 with respect to $\tilde{b}$ in that range then comes from the variation of $\langle n_\pi(\tilde{b})\rangle$, $\langle (n_\pi(\tilde{b}))^2\rangle$, and from $\rho(q,\tilde{b})$. With Eq. (4.72), $R(\tilde{k}_1,\tilde{k}_2)$ is given by Eq. (4.66) with $D(\tilde{k})$ replaced by $D_B(\tilde{k})$ and $\rho(q)$ replaced by $\langle \rho(q)\rangle_B$.

In practice, to maximize $D_B(k)$, we must select a narrow range of b around $b=0$ by measuring P_1 and P_2 with additional constraints on the distribution of the remaining fragments produced in the nuclear collision. To isolate such desired central collisions, high associated (charged or pion) multiplicities, together with approximate azimuthal symmetry may be required.[19]

This concludes our discussion of the effects of different production dynamics on $R(\tilde{k}_1,\tilde{k}_2)$. We turn next to the question of how final state interactions can distort the interference pattern resulting from a given production mechanism.

V. FINAL STATE INTERACTIONS

A. Graphical Analysis

In Section IV, we considered a model of pion production and absorption for nuclear collisions which is based on an interaction part of the action functional of the form

$$S_J = \int d^4x\, J(x)\phi(x) \quad , \tag{5.1}$$

where ϕ is the pion Heisenberg field and $J(x)$ is a classical source current. Equation (4.6) follows immediately from Eq. (5.1), and in the interaction picture I, $\langle \tilde{k}|S_J|0\rangle = J(\tilde{k})$, given by Eq. (4.8), is the amplitude to create one pion of momentum $\tilde{k}$ as illustrated in Fig. 1.

The amplitude S_{00} for no pions to be produced can be evaluated using Wick's theorem in the interaction picture[31] as

$$\begin{aligned} S_{00} &= \langle 0|T(\exp i\int d^4x\, J(x)\phi_I(x))|0\rangle \\ &= \exp\{-\frac{i}{2}\int d^4x\, d^4y\, J(x)\,\Delta_F(x-y)J(y)\} \\ &= \exp\left\{-\frac{i}{2}\int \frac{d^4k}{(2\pi)^4}\,\frac{|J(\tilde{k},k_o)|^2}{k_o^2 - |\tilde{k}|^2 - m_\pi^2 + i\varepsilon}\right\} \\ &= e^{-\bar{n}/2}\, e^{i\chi_J} \end{aligned} \tag{5.2}$$

where $i\Delta_F(x-y) = \langle 0|T(\phi_I(x)\phi_I(y))|0\rangle$ is the Feynman pion propagator, $\bar{n}$ is given by Eq. (4.9), and the real phase χ_J is given by the principal value integral

$$\chi_J = -\tfrac{1}{2}\, P\int \frac{d^4k}{(2\pi)^4}\,\frac{|J(\tilde{k},k_o)|^2}{k^2 - m_\pi^2} \quad . \tag{5.3}$$

Note that $J(\tilde{k},k_o)$ is the usual Fourier transform of $J(\tilde{x},t)$ and related to $J(\tilde{k})$ in Eq. (4.8) via $J(\tilde{k},\omega_k)((2\pi)^3\, 2\omega_k)^{-1/2} = J(\tilde{k})$.

Equation (5.2) can be simply interpreted in terms of Feynman diagrams. First we recall that the Linked Cluster Theorem asserts that $\log S_{00}$ is equal to the sum of all connected graphs in the theory. For Eq. (5.1), there is only one connected diagram, $\otimes\!\!\rightarrow\!\!\otimes$, whereby a pion is created at some point x and destroyed at some other point y. The value of the diagram is precisely $-\bar{n}/2 + i\chi_J$ as computed above.

The amplitude to produce exactly m pions with momenta $\tilde{k}_1,\ldots,\tilde{k}_m$ is

$$S(\tilde{k}_1,\ldots,\tilde{k}_m) = \langle \tilde{k}_1\ldots\tilde{k}_m \left| T\left(\exp i\int d^4x\, J(x)\,\phi_I(x)\right) \right| 0\rangle$$

$$= iJ(\tilde{k}_1)\ldots iJ(\tilde{k}_m)\, e^{-\bar{n}/2+i\chi_J} \quad , \tag{5.4}$$

which is what we also get by evaluating the Feynman diagrams in Fig. 3.

We can now recover the previous result, Eq. (4.14), for the m-pion inclusive from

$$P_m(\tilde{k}_1,\ldots,\tilde{k}_m) = \sum_{n=m}^{\infty} \frac{1}{(n-m)!}\int d^3k_{m+1}\ldots d^3k_n \; |S(\tilde{k}_1,\ldots,\tilde{k}_n)|^2 \; . \tag{5.5}$$

In this model, P_m is obtained by simply squaring the diagram in Fig. 3a.

Now we turn to the effects of final state interactions. To incorporate such interactions, we introduce effective one- and two-body potentials, $V(x)$ and $U(x-y)$, via the following action functionals

$$S_V = -\tfrac{1}{2}\int d^4x\; \phi(x)V(x)\phi(x) \quad , \tag{5.6}$$

and

$$S_U = -\tfrac{1}{8}\int d^4x\; d^4y\; \phi^2(x)\,U(x-y)\phi^2(y) \quad . \tag{5.7}$$

The optical potential V (dimensions m^2) describes the interaction of the produced pions with the nuclear system. The $\pi\pi$ final state interactions

are to be described via U (dimensions m^4) in Eq. (5.7). For Coulomb final state interactions, Eqs. (5.6) and (5.7) are modified in the usual way to take into account the four-vector nature of the Coulomb field $A_\mu(x)$.

Introducing S_V and S_U in addition to S_J obviously modifies the pion production amplitudes. In Fig. 4 typical final state distortion diagrams are shown. In Fig. 4a, two pions are produced at space-time points x and y with amplitude $J(x)J(y)$. The pions then scatter in the external potential $V(x_i)$ at arbitrary points x_i, and they also scatter off each other via U before being detected with momentum $\tilde{k}_1$ and $\tilde{k}_2$. What greatly complicates the problem is the two-body potential U which also leads to interactions with virtual pions which are produced and reabsorbed during the nuclear collision as illustrated in Fig. 4b. In contrast, the distortion graphs due to the one-body optical potential, V, illustrated in Fig. 4c, can be easily summed. We turn in the next section to that special case, when S_U can be ignored compared to S_V.

B. One-Body Optical Potential Case

1. Coherent state distortions

To sum all rescattering diagrams in Fig. 4c due to an optical potential V, we need only to solve for the pion propagation $i\Delta_V(x,y) = \langle 0|T(\phi_V(x)\,\phi_V(y))\,|0\rangle$, in the Furry picture [see p.566-575 of Ref. 35] in which the field $\phi_V(x)$ satisfies

$$(\Box + m_\pi^2 + V(x))\,\phi_V(x) = 0 \quad . \tag{5.8}$$

Then Δ_V satisfies the integral equation

$$\Delta_V(x,y) = \Delta_o(x-y) + \int d^4z\; \Delta_o(x-z)V(z)\Delta_V(z,y) \quad , \tag{5.9}$$

with Δ_o being the free Feynman propagator. In terms of Δ_V, we can sum all disconnected diagrams to obtain for the vacuum-to-vacuum amplitude

$$S_{00}(V) = \exp\left\{-i/2\int d^4x\ d^4y\ J(x)\Delta_V(x,y)J(y)\right\} e^{i\theta_V}\ , \qquad (5.10)$$

which is the natural extension of Eq. (5.2). In Eq. (5.10), there is an additional phase, θ_V, arising from virtual pair production and annihilation in the potential $V(x)$. The expression for θ_V involves a coupling constant integration over $\int V(x)\Delta_V(x,x)d^4x$, which we do not display since we will only be interested in $|S_{00}(V)|^2$. We assume that $V(x)$ is not strong enough to produce real pion pairs and hence that θ_V is real. This assumption is quite reasonable for the final state interaction potentials involved in nuclear collisions, and indeed, called for by the very definition of final state interactions. Only the external source current, $J(x)$, produces real pions in our case.

Therefore, the probability that no pions are produced in the reaction is

$$|S_{00}(V)|^2 = \exp\left\{-\int d^4x\ d^4y\ J(x)\ \mathrm{Re}\{\, i\Delta_V(x,y)\,\}\, J(y)\right\}$$
$$\equiv e^{-\bar{n}_V}\ . \qquad (5.11)$$

As we will see below, under the assumption that $V(x)$ does not lead to real pair production and the assumption that $V(x)$ supports no bound states, the number $\bar{n}_V$ defined via Eq. (5.11) will turn out to be the average pion multiplicity.

Now, we compute the amplitude, $iJ_V(\tilde{k})$, to produce one pion of momentum $\tilde{k}$ with no vacuum fluctuations as illustrated in Fig. 4c. For the case V=0, we already saw that $J_{V=0}(\tilde{k})$ is given by Eq. (4.8).

For $V \neq 0$, we compute J_V in the (out) interaction picture using standard techniques [see p.146-149, 178-189 of Ref. 31]

$$
\begin{aligned}
iJ_V(\tilde{k}) &= \langle \tilde{k}_{out} | 0_{in} \rangle / \langle 0_{out} | 0_{in} \rangle \\
&= \int d^3x \; f^*_{\tilde{k}}(x) \; i\overleftrightarrow{\partial}_o \langle 0_{out} | \phi_{out}(x) | 0_{in} \rangle \; S^{-1}_{00}(V) \\
&= \lim_{x_o \to \infty} \int d^3x \; f^*_{\tilde{k}}(x) \; i\overleftrightarrow{\partial}_o \langle 0_{out} | \phi_{out}(x) S | 0_{out} \rangle_{connected} \\
&= \lim_{x_o \to \infty} \int d^3x \; f^*_k(x) \; i\overleftrightarrow{\partial}_o \\
&\times \left\{ \sum_{n=0}^{\infty} \frac{i}{n!} \left(\frac{-i}{2}\right)^n \int d^4z_1 \ldots d^4z_n \; d^4y \; J(y) \right. \\
&\times \langle 0_{out} \Big| T(\phi_{out}(x)\phi_{out}(z_1)V(z_1)\phi_{out}(z_1) \ldots \\
&\times \left. \phi_{out}(z_n)V(z_n)\phi_{out}(z_n)\phi_{out}(y)) \Big| 0_{out} \rangle_{connected} \right\} \\
&= \lim_{x_o \to \infty} \sum_{n=0}^{\infty} i(-i)^n \int d^3x \; f^*_k(x) i\overleftrightarrow{\partial}_o \int d^4z_1 \ldots d^4z_n \; d^4y \; J(y) \\
&\times \left\{ i\Delta_o(x-z_1)V(z_1)i\Delta_o(z_1-z_2) \; \ldots \; V(z_n)i\Delta_o(z_n-y) \right\} \\
&= i \int d^4y \; J(y) (\psi^-_{\tilde{k}}(y))^* \qquad , \qquad (5.12)
\end{aligned}
$$

where in standard notation,[31] $f^*_k(x) = e^{ikx}/\sqrt{(2\pi)^3 2\omega_k}$, $\overleftrightarrow{\partial}_o = \overrightarrow{\partial}_o - \overleftarrow{\partial}_o$, and S is the S-matrix for the combined interaction S_J and S_V in Eqs. (5.1) and (5.6). We have also defined the incoming scattering wavefunction

$$(\psi^-_{\tilde{k}}(x))^* = \lim_{y_o \to \infty} \int d^3y\ f^*_{\tilde{k}}(y) \overleftrightarrow{i\partial}_{y_o}\ i\Delta_V(y,x)$$

$$= \int d^3y\ f^*_{\tilde{k}}(y) \overleftrightarrow{i\partial}_{y_o} \langle 0|T(\phi_{out}(y)\phi_V(x))|0\rangle$$

$$= \langle \tilde{k}_{out}|\phi_V(x)|0\rangle \quad . \tag{5.13}$$

In Eq. (5.13), the second line follows from the definition of Δ_V in terms of the Furry picture fields, ϕ_V, and from the asymptotic weak convergence of ϕ_V to the non-interacting out-field ϕ_{out}.

From Eq. (5.8) we see then that $\psi^-_{\tilde{k}}$ satisfies

$$(\Box + m^2 + V(x))\psi^-_{\tilde{k}}(x) = 0 \tag{5.14}$$

together with the boundary condition that

$$\lim_{x_o \to +\infty} \psi^-_{\tilde{k}}(x) = f_{\tilde{k}}(x) \equiv \frac{e^{-ikx}}{\sqrt{(2\pi)^3\ 2\omega_k}} \quad . \tag{5.15}$$

Thus ψ^-_k reduces to a plane wave at $x_o \to \infty$. Naturally, ψ^-_k also reduces to f_k in the case $V \to 0$. Note that we have implicitly used in Eq. (5.13) the assumption that the vacuum $|0\rangle$ is stable with respect to the interaction S_V in Eq. (5.6). This can be seen from the first line of Eq. (5.13) since, in general, both positive and negative energy solutions of Eq. (5.14) contribute to $\Delta_V(x,y)$. Equation (5.15) only follows when the negative energy solutions do not contribute in the $y_o \to \infty$ limit, i.e., no pair production occurs.

Under this same assumption we can write

$$i\Delta_V(x,y) = \int d^3k \Big\{ \theta(x_o - y_o) \langle 0|\phi_V(x)|\tilde{k}_{out}\rangle \langle \tilde{k}_{out}|\phi_V(y)|0\rangle$$

$$+ \theta(y_o - x_o) \langle 0|\phi_V(y)|\tilde{k}_{out}\rangle \langle \tilde{k}_{out}|\phi_V(x)|0\rangle \Big\} \tag{5.16}$$

since ϕ_V connects then only one particle state to the vacuum. Actually, Eq. (5.16) also requires that $V(x)$ does not support bound states, i.e., only continuum one-particle intermediate states contribute. This latter requirement should also be well satisfied in nuclear collisions.

Summarizing Eqs. (5.12) and (5.13), we have obtained the intuitive result

$$J_V(\tilde{k}) = \int d^4x\, J(x) \langle \tilde{k}_{out} | \phi_V(x) | 0 \rangle \quad , \tag{5.17}$$

which states that the amplitude to observe one pion with momentum $\tilde{k}$ is the product of the amplitude $J(x)$ for creating a pion at some space-time point x times the amplitude, $\langle \tilde{k}_{out} | \phi_V(x) | 0 \rangle$, for propagating that pion from x such that its wavefunction approaches a plane wave as $t \to +\infty$.

We can now immediately calculate the amplitude for creating exactly m-pions as

$$S(\tilde{k}_1, \ldots, \tilde{k}_m) = iJ_V(\tilde{k}_1) \ldots iJ_V(\tilde{k}_m)\, S_{00}(V) \quad , \tag{5.18}$$

with the vacuum fluctuation amplitude $S_{00}(V)$ given by Eq. (5.10). To calculate the m-pion inclusive distribution via Eq. (5.5) we need to evaluate

$$\begin{aligned} \int |J_V(k)|^2 d^3k &= \int d^4x d^4y\, J(x) J(y) \left\{ \int d^3k \, \langle 0 | \phi_V(x) | k_{out} \rangle \langle k_{out} | \phi_V(y) | 0 \rangle \right\} \\ &= \int d^4x d^4y\, J(x)\, \mathrm{Re}\left(i\Delta_V(x,y)\right) J(y) \\ &= \bar{n}_V \quad , \end{aligned} \tag{5.19}$$

which follows from Eqs. (5.17)(5.16)(5.11).

Using Eqs. (5.18) and (5.19) in Eq. (5.5), we obtain finally

$$P_m(\tilde{k}_1,\ldots,\tilde{k}_m) = |J_V(\tilde{k}_1)|^2 \ldots |J_V(\tilde{k}_m)|^2 \quad , \tag{5.20}$$

which is the natural generalization of Eq. (4.14). Integrating the single pion inclusive distribution (m=1) shows immediately that $\bar{n}_V$ in Eq. (5.19) is the mean pion multiplicity.

Equation (5.20) demonstrates that for a pure current source, the only effect of the external potential is to redistribute the momentum distribution of pions without introducting correlations. This is clear from the diagrammatic analysis. The resulting correlation function is thus identical to Eq. (4.15).

2. Chaotic field distortions

Now consider a chaotic ensemble of currents as in Eq. (4.47). The on-shell Fourier transform $J_{ch}(\tilde{k})$ is now replaced by

$$\begin{aligned} J^V_{ch}(\tilde{k}) &= \int d^4x \, (\psi^-_{\tilde{k}}(x))^* \sum_{i=1}^{N} e^{i\phi_i} J_\pi(x-x_i) \\ &= \int \frac{d^4q}{(2\pi)^4} \, \psi^{-*}_{\tilde{k}}(q) \, J_\pi(q) \sum_{i=1}^{N} e^{i\phi_i} \, e^{iqx_i} \quad , \end{aligned} \tag{5.21}$$

in terms of the space-time Fourier transforms

$$\psi^-_{\tilde{k}}(q) \equiv \int e^{iqx} \, \psi^-_{\tilde{k}}(x) \, d^4x \quad , \tag{5.22}$$

and

$$J_\pi(q) = \int e^{iqx} \, J(x) d^4x \quad . \tag{5.23}$$

Note that in the limit $V \to 0$, $\psi^-_{\tilde{k}}(x) \to f_{\tilde{k}}(x)$ as in Eq. (5.15), and therefore

$$\bar{\psi}_{\tilde{k}}(q) \xrightarrow[V\to 0]{} (2\pi)^4\, \delta(q_o - \omega_k)\, \delta^3(\tilde{q} - \tilde{k})\, \frac{1}{\sqrt{(2\pi)^3\, 2\omega_k}} \quad . \tag{5.24}$$

In that same limit, $J^V_{ch}(\tilde{k})$ reduces to Eq. (4.47).

We can now evaluate the ensemble average over $\{N, \phi_i, x_i\}$ for $P_1(\tilde{k})$ as in Eq. (4.60),

$$\begin{aligned} P_1(\tilde{k}) &= \langle\, |J^V_{ch}(\tilde{k})|^2 \,\rangle_{\{N,\phi_i,x_i\}} \\ &= \langle N \rangle \int \frac{d^4q}{(2\pi)^4}\, \frac{d^4q'}{(2\pi)^4}\, \bar{\psi}^*_{\tilde{k}}(q) \left\{ J_\pi(q)\, \rho(q-q')\, J^*_\pi(q') \right\} \bar{\psi}_{\tilde{k}}(q') \ , \end{aligned} \tag{5.25}$$

where $\rho(q)$ is the space-time Fourier transform of the chaotic source distribution $\rho(x)$ in Eq. (4.29).

To simplify Eq. (5.25), we note that according to Eq. (5.24), $\bar{\psi}_{\tilde{k}}(q)$ must be sharply peaked around $q_o = \omega_k$ and $\tilde{q} = \tilde{k}$. The "width" of $\bar{\psi}_{\tilde{k}}(q)$ around $q = (\omega_k, \tilde{k})$ of course depends on the strength and form of the external potential $V(x)$. It is clear that the average value $\langle V \rangle$ of the external potential must set the scale of the width of $\bar{\psi}_{\tilde{k}}(q)$. On the other hand, $J_\pi(q)$ varies on a scale $\gtrsim m_\pi$. Thus, if $\langle V \rangle \ll m_\pi^2$, then $J_\pi(q)$ varies slowly compared to $\bar{\psi}_{\tilde{k}}(q)$, and we can approximate

$$\bar{\psi}^*_{\tilde{k}}(q)\, J_\pi(q) \approx \bar{\psi}^*_{\tilde{k}}(q)\, J_\pi(\tilde{k}, \omega_k) \quad . \tag{5.26}$$

When Eq. (5.26) holds, Eq. (5.25) simplifies to

$$P_1(\tilde{k}) \approx |J_\pi(\tilde{k})|^2 \langle N \rangle\, \rho_V(\tilde{k}, \tilde{k}) \quad , \tag{5.27}$$

where $J_\pi(\tilde{k})$ is given by Eq. (4.8), and the <u>distorted</u> transform of $\rho(x)$ is defined as (note convention about $\sqrt{(2\pi)^3\, 2\omega_k}$ factors)

$$\rho_V(\tilde{k}_1,\tilde{k}_2) = \int \frac{d^4q}{(2\pi)^4}\,\frac{d^4q'}{(2\pi)^4}\,\sqrt{(2\pi)^3 2\omega_{k_1}}\;\psi^{-*}_{\tilde{k}_1}(q)\,\rho(q-q')\;\psi^{-}_{\tilde{k}_2}(q')\,\sqrt{(2\pi)^3 2\omega_{k_2}}$$

$$= \int d^4x\;\rho(x)\;\left(\psi^{-}_{\tilde{k}_1}(x)\right)^*\;\psi^{-}_{\tilde{k}_2}(x)\;(2\pi)^3\sqrt{2\omega_{k_1}2\omega_{k_2}}\quad . \qquad (5.28)$$

From Eq. (5.24), the distorted transform reduces to the Fourier transform when $V\to 0$, i.e.,

$$\rho_V(\tilde{k}_1,\tilde{k}_2) \xrightarrow[V\to 0]{} \rho(\tilde{k}_1-\tilde{k}_2,\;\omega_1-\omega_2)\quad . \qquad (5.29)$$

Thus $\rho_V(\tilde{k},\tilde{k}) \to 1$ in that limit, and Eq. (5.27) reduces then to Eq. (4.35).

For $\tilde{k}_1=\tilde{k}_2$, $\rho_V(\tilde{k}_1,\tilde{k}_2)$ has the simple interpretation of being the probability to find the pion in the interaction region specified by $\rho(x)$ given that it was measured at $t\to\infty$ in state $|\tilde{k}\rangle$. For a repulsive potential, $|\psi^-_k|^2 < 1$ for small x and hence $\rho_V(\tilde{k},\tilde{k}) < 1$. Thus $\rho_V(\tilde{k},\tilde{k})$ can be thought of as a penetration probability through the external final state interaction potential.

Evaluating next the double pion inclusive distribution in the approximation where Eq. (5.26) holds and $\langle N\rangle \gg 1$, we get

$$P_2(\tilde{k}_1,\tilde{k}_2) = \langle |J^V_{ch}(\tilde{k}_1)|^2 |J^V_{ch}(\tilde{k}_2)|^2 \rangle_{\{N,\phi_i,x_i\}}$$

$$\approx |J_\pi(\tilde{k}_1)|^2 |J_\pi(\tilde{k}_2)|^2 \langle N\rangle^2$$

$$\times \left\{\rho_V(\tilde{k}_1,\tilde{k}_1)\rho_V(\tilde{k}_2,\tilde{k}_2) + |\rho_V(\tilde{k}_1,\tilde{k}_2)|^2\right\}\quad . \qquad (5.30)$$

In this chaotic field limit, we therefore obtain the following expression for the two-pion correlation function:

$$R(\tilde{k}_1,\tilde{k}_2) \approx 1 + \frac{|\rho_V(\tilde{k}_1,\tilde{k}_2)|^2}{\rho_V(\tilde{k}_1,\tilde{k}_1)\rho_V(\tilde{k}_2,\tilde{k}_2)} \quad . \tag{5.31}$$

Noting Eq. (5.28), we can rewrite this expression in analogy to the simple form in Eq. (3.6) as

$$R(\tilde{k}_1,\tilde{k}_2) = \frac{\int d^4x d^4y\ \rho(x)\rho(y)\ \left|\frac{1}{\sqrt{2}}\left(\psi^-_{\tilde{k}_1}(x)\psi^-_{\tilde{k}_2}(y) + \psi^-_{\tilde{k}_2}(x)\psi^-_{\tilde{k}_1}(y)\right)\right|^2}{\int d^4x d^4y\ \rho(x)\rho(y)\ |\psi^-_{\tilde{k}_1}(x)|^2|\psi^-_{\tilde{k}_2}(y)|^2} . \tag{5.32}$$

In the numerator the symmetrized two-pion amplitude appears, whereas in the denominator the unsymmetrized amplitude appears. This is the expected form of the correlation function for the chaotic field case based on the heuristic arguments in Section III. Our derivations have the advantage of showing the conditions necessary to derive Eq. (5.32) in an exactly solvable field theoretic model specified by Eqs. (5.1, 5.6).

3. Partially coherent case

For this more general case, the current in Eq. (5.12) is written in analogy to Eq. (4.57) as

$$J_V(\tilde{k}) = J^V_o(\tilde{k}) + J^V_{ch}(\tilde{k}) \tag{5.33}$$

with J^V_{ch} given by Eq. (5.21) and J^V_o given by Eq. (5.12) with $J(x) = J_o(x)$.

Evaluating the single-pion inclusive distribution gives

$$P_1(\tilde{k}) = \langle |J^V_o(\tilde{k}) + J^V_{ch}(\tilde{k})|^2 \rangle_{\{N,\phi_i,x_i\}}$$

$$= n_o(\tilde{k},V) + n_{ch}(\tilde{k},V) \quad , \tag{5.34}$$

with $n_{ch}(\tilde{k},V)$ given by Eq. (5.27) and $n_o \equiv |J_o^V|^2$. Note that the degree of coherence, Eq. (4.65), is affected by final state interactions. The distorted degree of coherence is given by

$$D_V(\tilde{k}) = \frac{n_o(\tilde{k},V)}{(n_o(\tilde{k},V) + n_{ch}(\tilde{k},V))} \quad . \tag{5.35}$$

Finally, evaluating the double inclusive distribution, the correlation function replacing Eq. (4.66) is found to be

$$R(\tilde{k}_1,\tilde{k}_2) \approx 1 + (1 - D_V(\tilde{k}_1))(1 - D_V(\tilde{k}_2)) \; |\bar{\rho}_V(\tilde{k}_1,\tilde{k}_2)|^2$$
$$+ [D_V(\tilde{k}_1)D_V(\tilde{k}_2)(1 - D_V(\tilde{k}_1))(1 - D_V(\tilde{k}_2))]^{\frac{1}{2}} \; 2\mathrm{Re}\; \bar{\rho}_V(\tilde{k}_1,\tilde{k}_2) \; , \tag{5.36}$$

where

$$\bar{\rho}_V(\tilde{k}_1,\tilde{k}_2) = \frac{\rho_V(\tilde{k}_1,\tilde{k}_2)}{(\rho_V(\tilde{k}_1,\tilde{k}_1)\rho_V(\tilde{k}_2,\tilde{k}_2))^{\frac{1}{2}}} \quad , \tag{5.37}$$

replaces the Fourier transform $\rho(k_1-k_2)$ in terms of the distorted transforms given by Eq. (5.28). Of course, in the limit $V \to 0$, Eq. (5.36) reduces to (4.66).

Note that the intercept $R(\tilde{k},\tilde{k}) = 2 - D_V^2(\tilde{k})$ measures the distorted degree of coherence. Also, it is clear that the geometrical information provided by $R(\tilde{k}_1,\tilde{k}_2)$ is distorted by final state interactions. For a general partially coherent field in the presence of final state interactions it is therefore a non-trivial task to unfold the effects of $V(x)$. In a subsequent paper,[21] we study systematically how to unfold final state interactions for potentials $V(x)$ appropriate for nuclear collisions.

Our aim here has been to display the structure of the relations between $R(\tilde{k}_1,\tilde{k}_2)$, $\rho(x)$, $D(\tilde{k})$, and $V(x)$ as summarized by Eq. (5.36).

C. Two-Body Final State Interactions

1. The Bethe-Salpeter amplitude

With the inclusion of a two-body potential U via Eq. (5.7), no exact calculation of final state distortions is possible. However, an important class of diagrams (Figs. 4a,4c) can be summed to obtain a reasonable approximation to such distortions.

The essential physical approximation is that the single-pion inclusive distribution, $P_1(\tilde{k})$, is not affected significantly by $U(x-y)$. This approximation is expected to be good when the single pion trajectories (wave functions) are determined mainly by the external potential $V(x)$. For Coulomb final state interactions the strength of the external potential $Z\alpha \sim 1$, is much larger than that of the relative potential, $\alpha \ll 1$. In this approximation, we therefore neglect the effect of two-body final state interactions between observed and unobserved pions as in Fig. 4b. Only diagrams summed in Fig. 4c are considered, i.e.,

$$P_1(\tilde{k}) \approx \langle |J_V(\tilde{k})|^2 \rangle \quad , \tag{5.38}$$

as given, for example, by Eq. (5.34) for partially coherent fields.

The double pion inclusive distribution, on the other hand, is clearly sensitive to the distortions of the relative wave function of the observed pion pair. This is especially true for small momentum transfers, $|\tilde{k}_1-\tilde{k}_2| \lesssim m_\pi \sqrt{\alpha}$, corresponding to classically forbidden regions of phase space. The class of diagrams that lead in the non-relativistic

limit to the two-body Schrodinger equations for potentials V and U is illustrated in Fig. 4a. Our second physical approximation is therefore to calculate the two-pion production amplitude $J_2(\tilde{k}_1,\tilde{k}_2)$ as in Fig. 4a. In this approximation then

$$J_2(\tilde{k}_1,\tilde{k}_2) = -\tfrac{1}{2}\int d^4x d^4y\ J(x)J(y)\ \langle \tilde{k}_1,\tilde{k}_2,\text{out}|T(\phi(x)\phi(y))|0\rangle_{4a} \quad , \quad (5.39)$$

where $\phi(x)$ is the Heisenberg field for the final state functionals $S_V + S_U$ in Eqs. (5.6) and (5.7), not including S_J.

In analogy to Eq. (5.13), we will denote the symmetrized two-pion scattering wavefunction appearing in Eq. (5.39) as

$$[\psi^-_{\tilde{k}_1,\tilde{k}_2}(x,y)]^* = \langle \tilde{k}_1,\tilde{k}_2,\text{out}|T(\phi(x)\phi(y))|0\rangle_{4a} \quad . \quad (5.40)$$

In order to sum all diagrams of the type in Fig. 4a, we first express $\psi^-_{k_1k_2}$ in terms of the two-pion propagator

$$G_2(x'y';xy) = (-i)^2\langle 0|T(\phi(x')\phi(y')\phi(x)\phi(y))|0\rangle$$

via the usual reduction procedure.[31] Then the Bethe-Salpeter ladder sum corresponding to Fig. 4a leads to the following integral equation for G_2:

$$G_2(x',y';x,y) = \left\{\Delta_V(x',x)\Delta_V(y',y) + \Delta_V(x',y)\Delta_V(y',x)\right\} + i\int d^4x''d^4y''\ G_2(x',y';x'',y'')U(x''-y'')\Delta_V(x'',x)\Delta_V(y'',y) \quad , \quad (5.41)$$

where we used $U(r) = U(-r)$ and the symmetry property of G_2 with respect to interchange of labels $x'' \leftrightarrow y''$.

From Eq. (5.41), we therefore obtain the Bethe-Salpeter integral

equation[36] for $\psi^-_{k_1k_2}$ as

$$\psi^-_{\tilde{k}_1,\tilde{k}_2}(x,y) = \phi^-_{\tilde{k}_1\tilde{k}_2}(x,y) - i\int d^4x''d^4x''\ \psi^-_{\tilde{k}_1,\tilde{k}_2}(x'',y'')U(x''-y'')\Delta^*_V(x'',x)\Delta^*_V(y'',y)\ , \tag{5.42}$$

where

$$\phi^-_{\tilde{k}_1,\tilde{k}_2}(x,y) = \psi^-_{\tilde{k}_1}(x)\psi^-_{\tilde{k}_2}(y) + \psi^-_{\tilde{k}_2}(x)\psi^-_{\tilde{k}_1}(y)\ , \tag{5.43}$$

is the asymptotic form of $\psi^-_{k_1,k_2}(x,y)$ with $\psi^-_{\tilde{k}}(x)$ given by Eq. (5.13), i.e.,

$$\lim_{\substack{x_0\to\infty\\ y_0\to\infty}} \psi^-_{\tilde{k}_1,\tilde{k}_2}(x,y) = \phi^-_{\tilde{k}_1,\tilde{k}_2}(x,y)\ . \tag{5.44}$$

Equations (5.42)-(5.44) show that $\psi^-_{k_1k_2}$ is the incoming two-pion scattering wavefunction in the potentials V(x) and U(x-y).

In differential form, it is straightforward to verify that

$$(\Box_x + m_\pi^2 + V(x))(\Box_y + m_\pi^2 + V(y))\psi^-_{\tilde{k}_1,\tilde{k}_2}(x,y) = -iU(x-y)\psi^-_{\tilde{k}_1,\tilde{k}_2}(x,y)\ . \tag{5.45}$$

In terms of this Bethe-Salpeter amplitude, the double-pion inclusive distribution in this approximation is given by

$$\begin{aligned} P_2(\tilde{k}_1,\tilde{k}_2) &\approx \langle\, |J_2(\tilde{k}_1,\tilde{k}_2)|^2 \rangle \\ &= \langle \tfrac{1}{4}\left|\int d^4x d^4y\ J(x)J(y)\ \psi^{-*}_{\tilde{k}_1,\tilde{k}_2}(x,y)\right|^2 \rangle\ . \end{aligned} \tag{5.46}$$

Note that in the limit where the two-body final state interactions are negligible ($U\equiv 0$), $\psi^-_{k_1k_2}$ reduces to $\phi^-_{k_1k_2}$ in Eq. (5.43), and

P_2 reduces to the external field distortion form in Eq. (5.20).

2. Gamow penetration factor

An extreme case of interest is when the external potential, V, can be neglected, and only the relative potential U contributes to final state distortions. In that case $\bar{\psi}_{k_1 k_2}$ can be decomposed into a product of a center of mass and relative wavefunction as

$$\bar{\psi}_{\tilde{k}_1,\tilde{k}_2}(xy) = \frac{e^{-iKR}\left\{\bar{\phi}_{q,K}(r) + \bar{\phi}_{q,K}(-r)\right\}}{(2\pi)^3 (2\omega_1 2\omega_2)^{\frac{1}{2}}}$$

$$\equiv \int \frac{d^4q'}{(2\pi)^4} \frac{e^{-iKR}\, e^{-iq'r}}{(2\pi)^3\sqrt{2\omega_1 2\omega_2}} \left\{\bar{\phi}_{q,K}(q') + \bar{\phi}_{q,K}(-q')\right\}, \tag{5.47}$$

where $K = k_1 + k_2$, $q = (k_1 - k_2)/2$, $x = R + r/2$, and $y = R - r/2$, and $\bar{\phi}_{q,K}(q')$ satisfies from Eq. 5.42

$$\bar{\phi}_{q,K}(q') = (2\pi)^4 \delta^4(q-q') - i\Delta_o^*\left(\frac{K}{2} + q'\right)\Delta_o^*\left(\frac{K}{2} - q'\right) \times \int \frac{d^4p}{(2\pi)^4}\, \bar{\phi}_{q,K}(p)\, U(q' - p) \quad , \tag{5.48}$$

with $\Delta_o^*(p) = (p^2 - m^2 - i\varepsilon)^{-1}$.

In the non-relativistic limit ($|\tilde{q}|, |\tilde{K}| \ll m_\pi$), the integral of $\bar{\phi}_{q,K}(q')$ over dq_o', which is $\bar{\phi}_{q,K}(\tilde{q}, t=0)$, satisfies the non-relativistic Lippmann-Schwinger equation.[36] The important point to note in Eq. (5.48) is that $\bar{\phi}_{q,K}(q')$ is sharply peaked around $q' = q$, with a width that is determined mainly by U(q-q'). This suggests that to a good approximation

$$J_2(\tilde{k}_1,\tilde{k}_2) = -\int \frac{d^4q'}{(2\pi)^4} \frac{J(K/2+q')\ J(K/2-q')}{(2\pi)^3\sqrt{2\omega_1\ 2\omega_2}} \tfrac{1}{2}\{\phi^-_{qK}(q') + \phi^-_{qK}(-q')\}^*$$

$$\approx iJ(\tilde{k}_1)iJ(\tilde{k}_2)\ (\phi^-_{qK}(r\equiv 0))^* \quad , \tag{5.49}$$

where $J(\tilde{k})$ is given by Eq. (4.8).

This approximation holds when $\phi^-_{q,K}(q')$ is sharply peaked compared to $J(q')$. In this case, the double pion inclusive distribuiton, Eq. (5.46), becomes approximately

$$P_2(\tilde{k}_1,\tilde{k}_2) \approx |\phi^-_{qK}(\tilde{r}=0,t=0)|^2 \langle |J(\tilde{k}_1)|^2|J(\tilde{k}_2)|^2\rangle \ . \tag{5.50}$$

For a partially coherent current ensemble, for example, the ensemble average is evaluated as in Eq. (4.61). Therefore, the effect of two-body final state interactions on the correlation function R is simply to multiply the correlation function in the absence of final state interactions (Eq. (4.63)) by a penetration factor

$$G(\tilde{k}_1,\tilde{k}_2) \equiv |\phi^-_{q,K}(\tilde{r}=0,t=0)|^2 \quad , \tag{5.51}$$

i.e.,

$$[R(\tilde{k}_1,\tilde{k}_2)]_U \approx G(\tilde{k}_1,\tilde{k}_2)\ [R(\tilde{k}_1,\tilde{k}_2)]_{U=0} \quad . \tag{5.52}$$

In the non-relativistic limit and for a Coulomb final state interaction, G is the well-known Gamow factor[21]

$$G(\tilde{k}_1,\tilde{k}_2) = 2\pi\eta/(e^{2\pi\eta} - 1) \ , \qquad \eta = \alpha m_\pi/|\tilde{k}_1-\tilde{k}_2| \ ,$$

which is the modulus square of the non-relativistic Coulomb wavefunction at the origin. In analogy to that Coulomb case we will refer to $G(\tilde{k}_1,\tilde{k}_2)$ as the Gamow penetration factor.

3. Distorted Born approximation and generalized Gamow factor

Up to now we have analyzed two special cases: (1) external one-body potential only, V(x), Eq. (5.20), and (2) relative two-body potential only, U(x-y), Eq. (5.50). The more general problem of combined one and two body final state interactions involves the solution of Eq. (5.42), which even in the non-relativistic limit is an extremely difficult task. The needed two pion amplitude $\psi^-_{\tilde{k}_1,\tilde{k}_2}$ in Eq. (5.46) is too complicated in practice to calculate, especially for Coulomb potentials. We can, however, obtain a reasonable estimate for $J_2(\tilde{k}_1,\tilde{k}_2)$ in Eq. (5.39) in the case that U is weak compared to V in the spirit of the distorted Born approximation.

From Eq. (5.42), $\psi^-_{\tilde{k}_1\tilde{k}_2} \approx \phi^-_{\tilde{k}_1\tilde{k}_2}$ to zeroth order in U. This means that in the distorted basis specified by $\phi^-_{\tilde{k}'_1,\tilde{k}'_2}$, the coefficients $C(\tilde{k}_1\tilde{k}_2,\tilde{k}'_1\tilde{k}'_2)$ in the expansion of $\psi^-_{\tilde{k}_1\tilde{k}_2}$ in that basis are peaked around $\tilde{k}'_1 = \tilde{k}_1$, $\tilde{k}'_2 = \tilde{k}_2$ and $\tilde{k}'_1 = \tilde{k}_2$, $\tilde{k}'_2 = \tilde{k}_1$. If U is weak compared to V then the width of $C(\tilde{k}_1\tilde{k}_2,\tilde{k}'_1\tilde{k}'_2)$ around those peaks will be small, and an approximation similar to that in Eq. (4.49) will be possible.

To develop this approximation we assume first that the time dependence of $V(x,t)$ is so slow that we can replace $V(x,t)$ by an effective time independent potential $V(\tilde{x})$. In that case the one-body distorted waves in Eq. (5.14) have the form

$$\psi^-_{\tilde{k}}(\tilde{x},t) = v^-_{\tilde{k}}(\tilde{x})\,\frac{e^{-i\omega_k t}}{\sqrt{2\omega_k(2\pi)^3}}\quad , \tag{5.53}$$

where $v^-_{\tilde{k}}(\tilde{x}) \to e^{i\tilde{k}\cdot\tilde{x}}$ as $|\tilde{x}| \to \infty$. These incoming scattering waves form a complete orthonormal basis in the potential $V(\tilde{x})$. Again we assume as in section V.B that $V(\tilde{x})$ supports no bound states. Inserting

Eq. (5.53) into Eq. (5.16), the external potential propagator can be decomposed into its positive and negative frequency parts as

$$\Delta_V(x',x) = \int \frac{d^4k}{(2\pi)^4} \frac{e^{-i\omega(x_o'-x_o)}}{2\omega_k} \left\{ \frac{v_{\tilde{k}}(\tilde{x}')\, v^*_{\tilde{k}}(\tilde{x})}{\omega - \omega_k + i\varepsilon} - \frac{v_{\tilde{k}}(\tilde{x})\, v^*_{\tilde{k}}(\tilde{x}')}{\omega + \omega_k - i\varepsilon} \right\}$$

$$\equiv \Delta_V^+(x',x) + \Delta_V^-(x',x) \quad . \tag{5.54}$$

To calculate the first order correction, $\delta\psi^-_{\tilde{k}_1\tilde{k}_2}$, to $\psi^-_{\tilde{k}_1\tilde{k}_2}$ from Eq. (5.42), we will neglect the negative frequency part, $\Delta_V^-(x',x)$, of $\Delta_V(x',x)$ because U is assumed so weak that virtual pair creation by U is negligible. Therefore, the first order correction, $\delta\psi^{-*}_{\tilde{k}_1\tilde{k}_2}$, from Eq. (5.42) is

$$\delta\psi^{-*}_{\tilde{k}_1\tilde{k}_2}(xy) \approx i \int d^4x' d^4y'\ \phi^{-*}_{\tilde{k}_1,\tilde{k}_2}(x',y') U(x'-y') \Delta_V^+(x',x) \Delta_V^+(y',y)$$

$$= i \int \frac{d^4k_1'}{(2\pi)^4} \frac{d^4k_2'}{(2\pi)^4}\ \Delta_o^+(k_1') \Delta_o^+(k_2')$$

$$\times \left\{ \langle\langle k_1 k_2 | U | k_1' k_2' \rangle\rangle + \langle\langle k_2 k_1 | U | k_1' k_2' \rangle\rangle \right\}$$

$$\times \frac{1}{(2\pi)^3 \sqrt{2\omega_1 2\omega_2}} \left\{ v^*_{\tilde{k}_1'}(\tilde{x})\, v^*_{\tilde{k}_2'}(\tilde{y})\ e^{ik_{10}'x_o}\ e^{ik_{20}'y_o} \right\}, \tag{5.55}$$

where $\Delta_o^+(k) \equiv (2\omega_k(k_o - \omega_k + i\varepsilon))^{-1}$, and the off-shell matrix element is defined as

$$\langle\langle k_1 k_2 | U | k_1' k_2' \rangle\rangle \equiv \int d^4x d^4y \left\{ v^*_{\tilde{k}_1}(\tilde{x}) v_{\tilde{k}_1'}(\tilde{x})\ e^{i(k_{10}-k_{10}')x_o} \right\}$$

$$\times\ U(x-y) \left\{ v^*_{\tilde{k}_2}(\tilde{y})\, v_{\tilde{k}_2'}(\tilde{y})\ e^{i(k_{20}-k_{20}')y_o} \right\} . \tag{5.56}$$

In the limit $V \to 0$, $v_{\tilde{k}}(\tilde{x}) \to e^{i\tilde{k}\cdot\tilde{x}}$ and

$$\langle\langle k_1 k_2 | U | k_1' k_2' \rangle\rangle \longrightarrow (2\pi)^4 \, \delta^4(k_1+k_2 - k_1'-k_2') \, U(k_1-k_1') \quad . \tag{5.57}$$

We can now evaluate the two-pion production amplitude, Eq. (5.39), to first order in U as

$$J_2(\tilde{k}_1,\tilde{k}_2) = iJ_V(\tilde{k}_1) iJ_V(\tilde{k}_2) + \delta J_2(\tilde{k}_1,\tilde{k}_2) \tag{5.58}$$

where

$$\delta J_2(\tilde{k}_1,\tilde{k}_2) = \int \frac{d^4k_1'}{(2\pi)^4} \frac{d^4k_2'}{(2\pi)^4} iJ_V(k_1') iJ_V(k_2') \frac{1}{(2\pi)^3 \sqrt{2\omega_1 2\omega_2}}$$

$$\times \left\{ i\Delta_o^+(k_1')\Delta_o^+(k_2') \langle\langle k_1 k_2 | U | k_1' k_2' \rangle\rangle \right\} \quad , \tag{5.59}$$

and the off-shell distorted transform $J_V(\tilde{k},k_o)$ is given by

$$J_V(\tilde{k},k_o) = \int d^4x \, e^{ik_o x_o} \, v_{\tilde{k}}^*(\tilde{x}) \, J(x) \quad . \tag{5.60}$$

Note that in our convention in Eq. (5.12), $J_V(\tilde{k}) = J_V(\tilde{k},\omega_k)((2\pi)^3 \, 2\omega_k)^{-1/2}$,

Using Eq. (5.57), it is easy to show that when $V \to 0$, Eqs. (5.58) and (5.59) agree with Eqs. (5.48) and (5.49) to first order in U, as they must.

We can now invoke the same approximation leading to Eq. (5.49), i.e., the function in the brackets in Eq. (5.59) is sharply peaked around $k_1'=k_1$, $k_2'=k_2$ compared to the slowly varying function $J_V(k_1')J_V(k_2')$. Therefore we obtain an approximate factorization as

$$\delta J_2(\tilde{k}_1,\tilde{k}_2) \approx iJ_V(\tilde{k}_1)iJ_V(\tilde{k}_2)\delta\phi^*(\tilde{k}_1,\tilde{k}_2) \quad , \tag{5.61}$$

where

$$\delta\phi^*(\tilde{k}_1,\tilde{k}_2) = i\int \frac{d^4k_1'}{(2\pi)^4}\,\frac{d^4k_2'}{(2\pi)^4}\,\Delta_o^+(k_1')\Delta_o^+(k_2')\langle\langle k_1k_2|U|k_1'k_2'\rangle\rangle \quad . \tag{5.62}$$

Finally, we obtain via Eqs. (5.46, 5.58, 5.61) the distorted Born approximation for the correlation function as

$$[R(\tilde{k}_1,\tilde{k}_2)]_{U,V} \approx \mathcal{G}(\tilde{k}_1,\tilde{k}_2)[R(\tilde{k}_1,\tilde{k}_2)]_{U=0,V} \quad , \tag{5.63}$$

where $\mathcal{G}$ is the generalized Gamow factor to first order in U but all orders in V,

$$\mathcal{G}(\tilde{k}_1,\tilde{k}_2) = 1 + 2\mathrm{Re}\,\delta\phi^*(\tilde{k}_1,\tilde{k}_2) \quad , \tag{5.64}$$

with $\delta\phi^*$ given by Eq. (5.62). In Eq. (5.63) $R_{U=0,V}$ is given for partially coherent fields by Eq. (5.36).

Equation (5.63) is the main result of section V, showing how both relative and external final state interactions affect the correlation function. If we consider V to be the external Coulomb field of strength $Z\alpha$, and U to be the relative Coulomb $\pi^-\pi^-$ potential of strength α, then Eq. (5.63) incorporates final state interaction to all orders in $(Z\alpha)$ but only first order in α. The numerical evaluation of Eq. (5.63) will be published elsewhere.[21] For a brief summary of those results refer back to Section I.

ACKNOWLEDGEMENTS

We are grateful to Drs. R. Stock, R. T. Poe, and K. M. Crowe for stimulating discussions on the experimental aspects of pion interferometry in nuclear collisions. Valuable discussions with Professor S. E. Koonin and Y. Karant on the theoretical aspects of the problem and useful comments on final state interactions by K. Gelbke are also gratefully acknowledged.

This work was supported by the Nuclear Science Division of the U. S. Department of Energy under contract No. W-7405-ENG-48.

REFERENCES

1. For a review of intensity interferometry in quantum optics, see, e.g., J.R.Klauder and E.C.G.Sudarshan, Fundamentals of Quantum Optics (W.A.Benjamin, Inc., New York, 1968).
2. M.L.Goldberger, H.W.Lewis, K.M.Watson, Phys. Rev. 132, 2764 (1963); 142, 25 (1966).
3. G.I.Kopylov, Phys. Lett. 50B, 572 (1974); G.I.Kopylov, M.J.Podgoretsky,[Yad. Fiz. 18, 656 (1973)] Sov. J. Nucl. Phys. 18, 336 (1974).
4. E.V.Shuryak, Phys. Lett. 44B, 387 (1973).
5. G.Cocconi, Phys. Lett. 49B, 459 (1974).
6. G.Goldhaber, S.Goldhaber, W.Lee, A.Pais, Phys. Rev. 120, 300 (1960).
7. F.Grard, et al., Nucl. Phys. B102, 221 (1976).
8. E.De Wolf, et al., "Bose-Einstein Effects in the Reaction $K^+p \to K^+p2\pi^+2\pi^-$ at 16 GeV/c," preprint (IIHE-76.11) (1976).
9. M.Deutschmann, et al., Nucl. Phys. B103, 198 (1976).
10. N.N.Biswas, et al., Phys. Rev. Lett. 37, 175 (1976).
11. C.Ezell, et al., Phys. Rev. Lett. 38, 873 (1977).
12. M.Deutschmann, et al., "A Study of the Bose-Einstein Interference for Pions Produced in Various Hadronic Interactions," CERN preprint (CERN/EP/PHYS 78-1), (January 1978).
13. G.N.Fowler, R.M.Weiner, Phys. Lett. 70B, 201 (1977); G.N.Fowler, N.Stelte, R.M.Weiner, "Condensation and Bose-Einstein Correlations," Univ. of Marburg preprint (September 1978).
14. A.Giovannini, G.Veneziano, "The Bose-Einstein Effect and the Jet Structure of Hadronic Final States," CERN preprint TH-2347 (July 1977).

15. J.Engels, K.Schillig, "Dynamical and Bose-Einstein Correlations of Centrally Produced Pion Pairs in Hadron-Hadron Collisions," CERN preprint TH-2401 (October 1977).

16. M.Gyulassy, Proceedings of the Symp. on Relativistic Heavy-Ion Collisions, GSI, Darmstadt, March 7-10, 1978; and LBL Report LBL-7704 (1978).

17. F.B.Yano, S.E.Koonin, Phys. Lett. 78B, 556 (1978).

18. For a review of models of nuclear collisions, see M.Gyulassy, Proceedings of Int. Symposium on Nuclear Collisions and Their Microscopic Description, Bled, Yugoslavia, September 1977 (Fizika 9: Suppl. 4, p.623); also see A.S.Goldhaber, H.H.Heckman, Ann. Rev. Nucl. Part. Sci. 28, 161 (1978).

19. S.Y.Fung, et al., Phys. Rev. Lett. 41, 1592 (1978).

20. K.M.Crowe, R.Stock, private communication.

21. Lance W.Wilson, M.Gyulassy, S.K.Kauffmann, "Pion Interferometry in Nuclear Collisions II: The Effect of Final State Interactions," LBL Report No. 8760 (1979).

22. D.Sivers, G.H.Thomas, Phys. Rev. D6, 1961 (1972).

23. D.Horn, R.Silver, Ann. Phys. 66, 509 (1971).

24. For a discussion on pion multiplicity distributions in nuclear collisions, see M.Gyulassy, S.K.Kauffmann, Phys. Rev. Lett. 40, 298 (1978); S.K.Kauffmann, M.Gyulassy, J. Phys. A11, 1715 (1978).

25. P.Grassberger, Nucl. Phys. B120, 231 (1977); Proceedings of the VIII Int. Symposium on Multiparticle Dynamics, Kaysersberg, France, June 1977, p.A-65.

26. G.H.Thomas, Phys. Rev. D15, 2636 (1977).

27. S.Y.Fung, et al., Phys. Rev. Lett. 40, 292 (1978).

28. M.Gyulassy, W.Greiner, Ann. Phys. 109, 485 (1977);
M.Gyulassy, Proceedings of the Topical Conf. on Heavy Ion Collisions, Fall Creek Falls, June 1977, p.457, and LBL Report No. 6525 (1977).

29. J.C.Botke, D.J.Scalapino, R.L.Sugar, Phys. Rev. D9, 813 (1974).

30. G.D.Westfall, et al., Phys. Rev. Lett. 37, 1202 (1976);
W.D.Myers, Nucl. Phys. A296, 177 (1978).

31. J.D.Bjorken and S.D.Drell, Relativistic Quantum Fields (McGraw-Hill, New York, 1965), pp.202-207.

32. A dynamical model leading to such charge-constrained coherent states has been recently constructed by S.K.Kauffmann and M.Gyulassy, in "Charge constrained coherent pion states produced in nuclear matter," LBL Report LBL-9011 (1979).

33. R.K.Smith, M.Danos, Proceedings of Topical Conf. on Heavy Ion Collisions, Fall Creek Falls, Conf-770602, p.363 (1977);
Z.Fraenkel, Y.Yariv, to be published;
J.D.Stevenson, Phys. Rev. Lett. 41, 1702 (1978).

34. Note also a recent derivation of the chaotic limit by E.A.Bartnik and K.Rzazewski, Phys. Rev. D18, 4308 (1978). Our derivation is more general in that corrections due to a finite number of source currents are considered.

35. S.S.Schweber, An Introduction to Relativistic Quantum Field Theory (Harper and Row, New York, 1962).

36. C.Schwartz and C.Zemach, Phys. Rev. 141, 1454 (1966).

APPENDIX A

SPACE-TIME PARAMETRIZATION FOR CHAOTIC FIELDS

1. Two-Pion Ensemble

In this section, we derive the chaotic field correlation function, Eq. (3.6), using a simple space-time parametrization of the pion density matrix. The model states in Eq. (4.5) will be chosen to be localized packets $|x_1, \ldots, x_n\rangle_f$ around space-time points x_i, which are assumed to be distributed in a space-time volume specified by $\rho(x)$.

We construct the normalizable, symmetrized packets via

$$|x_1, \ldots, x_n\rangle_f = \phi_f^+(x_1) \ldots \phi_f^+(x_n)|0\rangle \quad , \tag{A.1}$$

where

$$\phi_f^+(x) = \int d^3k \, \frac{e^{ikx}}{\sqrt{(2\pi)^3}} \, f(\tilde{k}) \, a^+(\tilde{k}) \quad , \tag{A.2}$$

with

$$kx = \omega_k x_o - \tilde{k}\cdot\tilde{x} \, , \quad \text{and} \quad [a(\tilde{k}), a^+(\tilde{k}')] = \delta^3(k-k') \, .$$

To insure that ${}_f\langle x|x\rangle_f = 1$, we normalize f such that

$$\int \frac{d^3k}{(2\pi)^3} \, |f(\tilde{k})|^2 = 1 \quad . \tag{A.3}$$

The two-pion state $|xy\rangle_f$ is then normalized to

$${}_f\langle xy|xy\rangle_f = 1 + \left|{}_f\langle x|y\rangle_f\right|^2 \quad , \tag{A.4}$$

with

$${}_f\langle x|y\rangle_f = [\phi_f(x), \phi_f^+(y)] = \int \frac{d^3k}{(2\pi)^3} \, e^{-ik(x-y)} \, |f(\tilde{k})|^2 \quad . \tag{A.5}$$

From Eqs. (A.3 - A.5), it follows that $1 \leq {}_f\langle xy|xy\rangle_f \leq 2$.

We can now construct a two-pion ensemble in this space-time picture as

$$\rho_\pi \approx N_f \int d^4x d^4y\ \rho(x)\rho(y)\ |xy\rangle_f\ {}_f\langle xy| \ , \tag{A.6}$$

where

$$\begin{aligned} N_f^{-1} &= \int d^4x\ d^4y\ \rho(x)\rho(y)\ {}_f\langle xy|xy\rangle_f \\ &= 1 + \int \frac{d^3k}{(2\pi)^3}\ \frac{d^3k'}{(2\pi)^3}\ \left| f(\tilde{k})\ \ \rho(\tilde{k}-\tilde{k}', \omega_k - \omega_{k'})\ f(\tilde{k}') \right|^2 \ . \end{aligned} \tag{A.7}$$

Clearly, $1 \leq N_f^{-1} \leq 2$ because $|\rho(q)|^2 \leq 1$.

The single inclusive distribution in this picture is obtained via Eqs. (4.2) and (A.6):

$$\begin{aligned} P_1(\tilde{k}) &= N_f \int d^4x d^4y\ \rho(x)\rho(y)\ {}_f\langle xy|a^+(\tilde{k})\, a(\tilde{k})\,|xy\rangle_f \\ &= N_f \int d^4x d^4y\ \rho(x)\rho(y) \int d^3k'\ |\langle \tilde{k}\tilde{k}'|xy\rangle_f|^2 \ , \end{aligned} \tag{A.8}$$

where

$$\langle \tilde{k}\tilde{k}'|xy\rangle_f = \left\{ e^{ikx}\, e^{ik'y} + e^{ik'x}\, e^{iky} \right\} \frac{f(\tilde{k}) f(\tilde{k}')}{(2\pi)^3} \ , \tag{A.9}$$

is the two-pion wavefunction in momentum space that is analogous to Ψ_{12} in Eq. (3.5). Evaluating Eq. (A.8), we find

$$P_1(\tilde{k}) = 2N_f \frac{|f(\tilde{k})|^2}{(2\pi)^3} \{1 + \varepsilon(\tilde{k})\} \ , \tag{A.10}$$

where $\varepsilon(\tilde{k})$ is a correction term given by

$$\varepsilon(\tilde{k}) = \int \frac{d^3k'}{(2\pi)^3}\ |f(\tilde{k}')|^2\ |\rho(k-k')|^2 \ , \tag{A.11}$$

which because $|\rho(q)|^2 \leq 1$ satisfies $0 \leq \varepsilon \leq 1$.

The double inclusive distribution with this parametrization is in turn given by

$$P_2(\tilde{k}_1,\tilde{k}_2) = 2N_f \frac{|f(\tilde{k}_1)|^2}{(2\pi)^3} \frac{|f(\tilde{k}_2)|^2}{(2\pi)^3} \{1 + |\rho(k_1-k_2)|^2\} . \quad (A.12)$$

Integrating Eqs. (A.10) and (A.12) and noting Eq. (A.7) we see that $\langle n_\pi \rangle = \langle n_\pi(n_\pi-1) \rangle = 2$ as it must be from Eq. (A.6). Therefore the correlation function, Eq. (1.1), which is to be compared to Eq. (3.6) is

$$\mathcal{R}(\tilde{k}_1,\tilde{k}_2) = \{1 + |\rho(k_1-k_2)|^2\}\{1 - \varepsilon(\tilde{k}_1,\tilde{k}_2)\} , \quad (A.13)$$

with a correction function given by

$$\varepsilon(\tilde{k}_1,\tilde{k}_2) = 1 - \{N_f(1+\varepsilon(\tilde{k}_1))(1+\varepsilon(\tilde{k}_2))\}^{-1} . \quad (A.14)$$

We show below that for nuclear collisions $\varepsilon << 1$ and, thus, that the ideal BE interference result, Eq. (3.6), follows in this simple space-time parametrization of ρ_π. Our aim in deriving Eq. (3.6) from Eq. (A.6) was to demonstrate that this form for the correlation function is a general consequence of a space-time picture of the production dynamics and not unique to the classical current ensemble derivation in Section IV.C. It is in fact straightforward (though tedious) to demonstrate that Eq. (3.6) also follows under suitable conditions from the more general space-time parametrization

$$\rho_\pi \approx \sum_n P_\pi(n) \int d^4x_1\rho(x_1) \ldots d^4x_n\rho(x_n) \; |x_1\ldots x_n\rangle_f \; {}_f\langle x_1\ldots x_n| , \quad (A.15)$$

with $P_\pi(n)$ being the pion multiplicity distribution. The necessary

condition to derive Eq. (3.6) from Eq. (A.15) is that the

pion wave packets be small compared to the dimensions of the reaction volume specified by $\rho(x)$.

2. Estimate of Correction Terms

Next we show that if the spatial extent, r_f, of the packet $|x\rangle_f$ is small compared to the spatial extent, R_o, of the pion source $\rho(x)$, then

$$\varepsilon \sim 0((r_f/R_o)^3) << 1 \qquad (A.16)$$

in both Eqs. (A.10) and (A.13). To see this we note first that Eq. (A.10) places a strong constraint on $|f(\tilde{k})|^2$ since the definition of the $\approx$ sign in Eq. (4.13) and (A.6) is that the right-hand side of both Eqs. (A.10) and (A.12) provide a good approximation to the observed inclusive distribution. Thus we are not free to choose $f(\tilde{k})$ as we like, but rather, Eq. (A.10) constrains $|f(\tilde{k})|^2$ to have a momentum dependence similar to the observed single pion inclusive distribution. Note the similarity between the role of f here and the classical current $J(k)$ in Section IV.

For relativistic nuclear collisions the observed pion distribution, and hence $|f(\tilde{k})|^2$ falls off rapidly for $|\tilde{k}| >> \langle k_\pi \rangle \sim m_\pi$. Therefore, we can estimate $r_f \sim \langle k_\pi \rangle^{-1} \sim 1$ fm. Next, from dimensional considerations of Eq. (A.3), we can estimate the order of magnitude $|f(\tilde{k})|^2$ for $|\tilde{k}| < 1/r_f$ as

$$\frac{|f(\tilde{k})|^2}{(2\pi)^3} \sim O(r_f^3) \sim O(m_\pi^{-3}) \quad . \tag{A.17}$$

On the other hand, for nuclear collisions, the dimensionless $\rho(k)$ satisfies $|\rho(k)| < 1$ and must fall off rapidly for $|\tilde{k}| > 1/R_o$, where $R_o \sim O(A^{1/3}\, m_\pi^{-1})$, A being the average nucleon number in the pion production region. For Eq. (2.1), A ~40. Therefore

$$\int d^3k' \; |\rho(k-k')|^2 \sim \int\limits_{|\tilde{k}-\tilde{k}'| \lesssim 1/R_o} d^3k' \sim O\left(\frac{1}{R_o^3}\right) \sim O\left(\frac{m_\pi^3}{A}\right) . \tag{A.18}$$

For $A \gg 1$, $|\rho(k)|^2$ is sharply peaked compared to $|f(\tilde{k})|^2$, and we finally obtain, for $k \lesssim 1/r_f$,

$$\varepsilon(\tilde{k}) \approx \frac{|f(\tilde{k})|^2}{(2\pi)^3} \int d^3k' \; |\rho(\tilde{k}-\tilde{k}', \omega_k - \omega_{k'})|^2$$

$$\sim O((r_f/R_o)^3) \sim O(1/A) \ll 1 \quad . \tag{A.19}$$

Note that for $k > 1/r_f$, $|f|^2$ and, hence, ε decreases rapidly.

Next, from Eq. (A.7)

$$N_f^{-1} = 1 + \int \frac{d^3k}{(2\pi)^3} \; |f(\tilde{k})|^2 \; \varepsilon(\tilde{k})$$

$$\leqslant 1 + \varepsilon(\tilde{k}) = 1 + O(1/A) \quad , \tag{A.20}$$

where we used Eq. (A.3) to obtain the upper bound on N_f^{-1} and then Eq. (A.19) to obtain the estimate for $\varepsilon(\tilde{k})$.

Equations (A.19) and (A.20) therefore imply that $\varepsilon(\tilde{k}_1, \tilde{k}_2)$ given by Eq. (A.14) is $O((r_f/R_o)^3) = O(1/A)$ as stated in Eq. (A.16).

Finally, we note that the same arguments leading to Eq. (A.20) can be made to estimate the correction term δ in Eq. (4.43) of section IV.C.1. In particular, comparing Eqs. (4.43) and (A.7), we see that we can identify

$$\delta = \frac{\langle N(N-1) \rangle}{\langle N^2 \rangle} \{N_f^{-1} - 1\} \tag{A.21}$$

where $|f(\tilde{k})|^2 = (2\pi)^3 |J_\pi(\tilde{k})|^2/\bar{n}_\pi$, with $\bar{n}_\pi$ given by Eq. (4.37). From Eq. (4.35), this $|f(\tilde{k})|^2$ is also constrained by the single pion inclusive distribution to decrease rapidly for $|\tilde{k}| \gtrsim m_\pi$. Thus, Eq. (A.17) still holds and the estimate for $N_f^{-1} - 1$ in Eq. (A.20) still holds. Therefore, $\delta = O(1/A)$ as stated in (4.43).

APPENDIX B

We derive here the limiting ensemble probability density for the chaotic current strength $|J_{ch}(\tilde{k})|^2$ to have the value $|J|^2$, Eq. (4.50). First define a vector pair of limiting random variables

$$(X(\tilde{k}),Y(\tilde{k})) = \lim_{N\to\infty} \left(\frac{P_1(\tilde{k})}{N}\right)^{\frac{1}{2}} \left(\sum_{i=1}^{N} \cos\theta_i \, , \sum_{i=1}^{N} \sin\theta_i\right) \quad , \tag{B.1}$$

where $\theta_i = kx_i + \phi_i$. The chaotic current strength, Eq. (4.49), is then given by

$$|J_{ch}(\tilde{k})|^2 = X^2(\tilde{k}) + Y^2(\tilde{k}) \quad . \tag{B.2}$$

The joint probability density of $(X(\tilde{k}),Y(\tilde{k}))$ is obtained as follows:

$$p(x,y;\tilde{k}) = \lim_{N\to\infty} \left\langle \delta\left(x - \left(\frac{P_1(\tilde{k})}{N}\right)^{\frac{1}{2}} \sum_{i=1}^{N} \cos\theta_i\right) \delta\left(y - \left(\frac{P_1(\tilde{k})}{N}\right)^{\frac{1}{2}} \sum_{i=1}^{N} \sin\theta_i\right)\right\rangle_{\{x_i,\phi_i\}}$$

$$= \lim_{N\to\infty} \frac{1}{(2\pi)^2} \int_{-\infty}^{\infty} du\, e^{-ixu} \int_{-\infty}^{\infty} dv\, e^{-iyv}$$

$$\times \left\langle \exp\left\{ i\left(\frac{P_1(\tilde{k})}{N}\right)^{\frac{1}{2}} \sum_{i=1}^{N} (u\cos\theta_i + v\sin\theta_i)\right\}\right\rangle_{\{x_i,\phi_i\}}$$

$$= \lim_{N\to\infty} \frac{1}{(2\pi)^2} \int_{-\infty}^{\infty} du\, e^{-ixu} \int_{-\infty}^{\infty} dv\, e^{-iyv}$$

$$\times \left[\int d^4x_1 \rho(x_1) \int_0^{2\pi} \frac{d\phi}{2\pi} \exp\left\{ i\left(\frac{P_1(\tilde{k})}{N}\right)^{\frac{1}{2}} (u\cos(kx_1+\phi) + v\sin(kx_1+\phi))\right\}\right]^N$$

$$= \lim_{N\to\infty} \left(\frac{1}{2\pi}\right)^2 \int_{-\infty}^{\infty} du\, e^{-ixu} \int_{-\infty}^{\infty} dv\, e^{-iyv} \left(1 - \frac{P_1(\tilde{k})}{4N}(u^2+v^2) + O\left(\frac{1}{N^{3/2}}\right)\right)^N$$

$$= \frac{1}{\pi P_1(\tilde{k})} \exp\left[\frac{-(x^2+y^2)}{P_1(\tilde{k})}\right] \quad . \tag{B.3}$$

We emphasize that we have implicitly incorporated the condition of Eq. (4.44), $N^{\frac{1}{2}}|\rho(k)| << 1$, via the device of averaging over the ϕ_i in obtaining Eq. (B.3). Now we write the probability density for $|J_{ch}(\tilde{k})|^2$ to have the value $|J|^2$, in terms of $p(x,y;\tilde{k})$:

$$P_{ch}(|J|^2;\tilde{k}) = \int_{-\infty}^{\infty} dx \int_{-\infty}^{\infty} dy\ \delta(|J|^2 - x^2 - y^2)\ p(x,y;\tilde{k}) \qquad (B.4)$$

from which Eq. (4.50) follows immediately.

We note that the bivariate Gaussian result for $p(x,y;\tilde{k})$ is simply an aspect of the Central Limit Theorem, as discussed in Ref. 1.

FIGURE CAPTIONS

Fig. 1. The amplitude M to produce two negative pions with momenta $\tilde{k}_1, \tilde{k}_2$ due to an ensemble of classical current sources $J_\pi(x - x_i)$ centered at space-time points x_i. These Feynman diagrams correspond to the amplitudes A_{ij} and B_j in Eqs. (4.39) and (4.40).

Fig. 2. Identical pion correlation function, Eq. (4.66), as a function of relative momentum $\tilde{q} = \tilde{k}_1 - \tilde{k}_2$ for fixed $\tilde{k} = (\tilde{k}_1 + \tilde{k}_2)/2$. The orientation of $\tilde{q}$ with respect to $\tilde{k}$ is held fixed at $\tilde{q}\cdot\tilde{k} = 0$, corresponding to equal energy pions ($|\tilde{k}_1| = |\tilde{k}_2|$). The effect of a finite degree of coherence $D(\tilde{k})$ is illustrated. The source of the chaotic component is assumed to be $\rho(\tilde{q}, q_o = 0) = \exp(-1/2\ q^2 R_o^2)$. Note that the effective radius Eq. (4.69) decreases with increasing coherence. Final state distortions are not taken into account.

Fig. 3. Feynman diagrams corresponding to the amplitude, Eq. (5.4), to produce (a) exactly m pions with (b) arbitrary vacuum fluctuation in the classical current model Eq. (5.2).

Fig. 4. (a) The amplitude $J_2(\tilde{k}_1, \tilde{k}_2)$, Eq. (5.39), to produce two pions including final state interactions with one- and two-body potentials V and U. (b) Scattering diagrams with virtual pions that are neglected in comparison with scattering diagrams (c) in the optical potential V. (c) The infinite class of diagrams summed via Eq. (5.9) and (5.12) to incorporate final state interactions with the optical potential V.

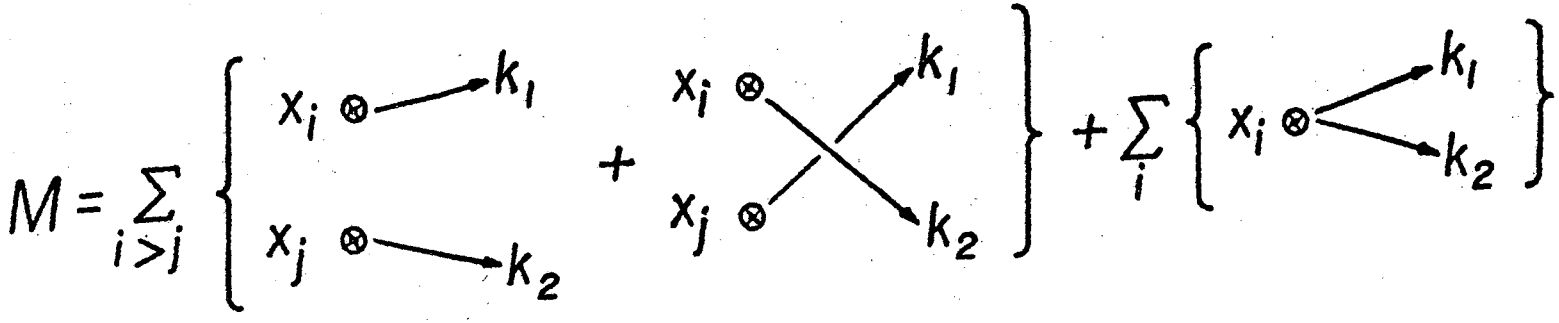

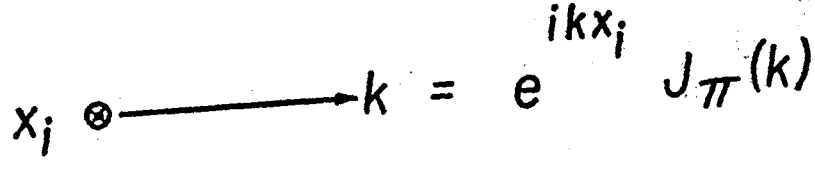

XBL 793-8708

Fig. 1

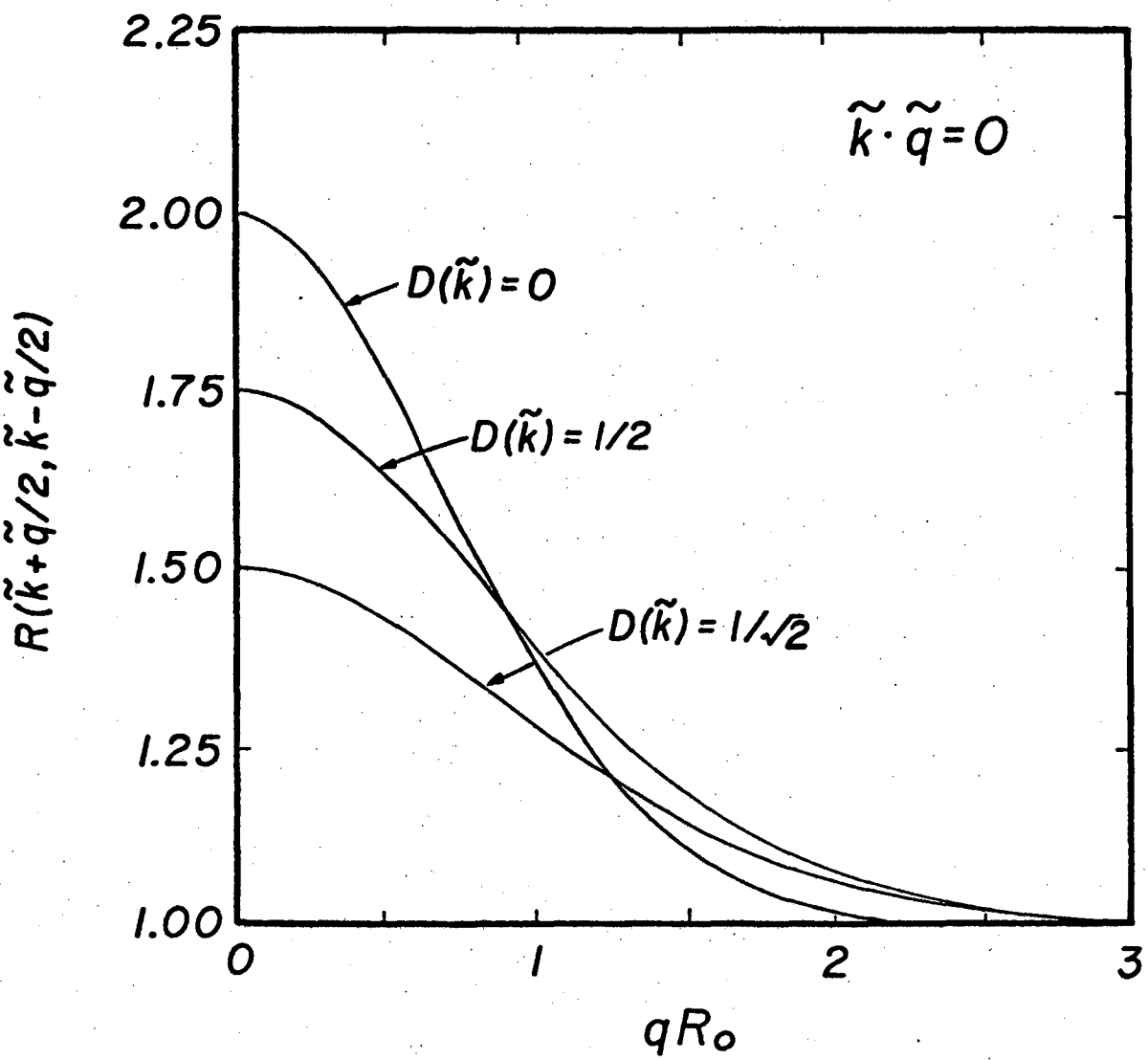

XBL 793-8709

Fig. 2

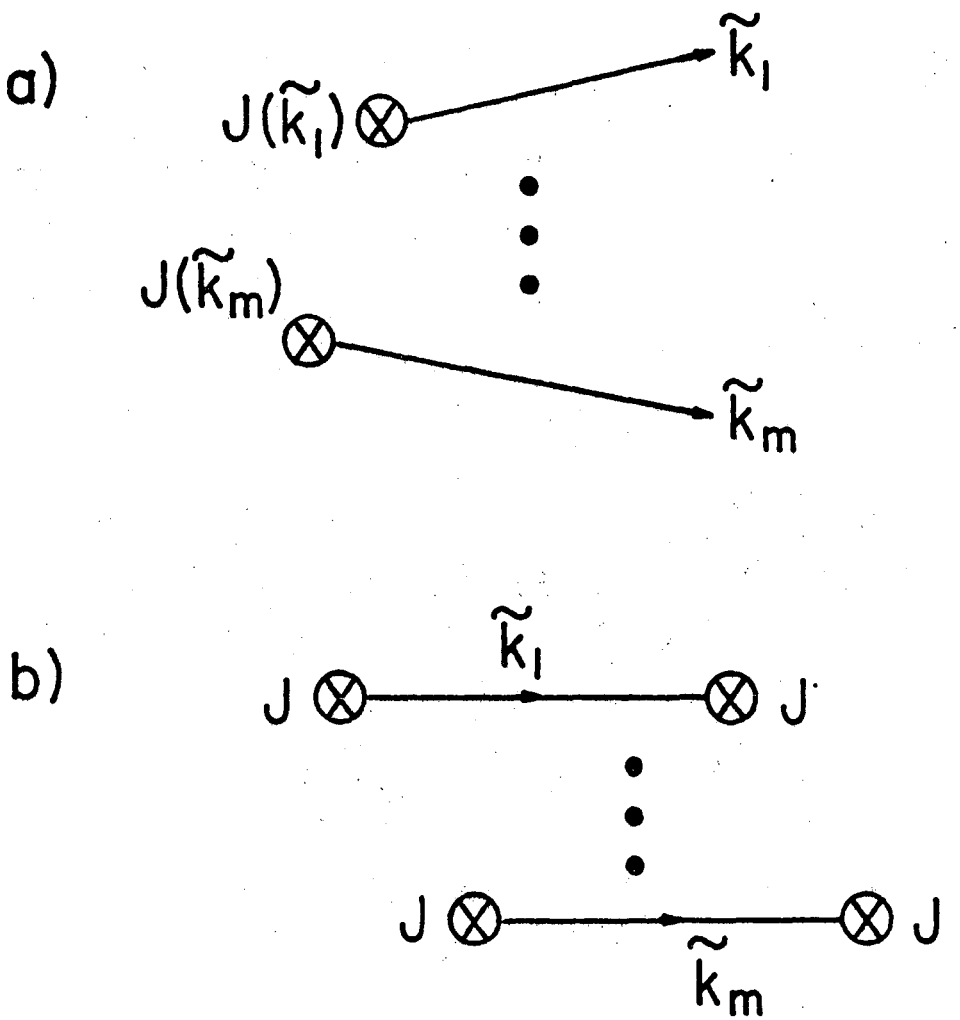

XBL 794-9243

Fig. 3

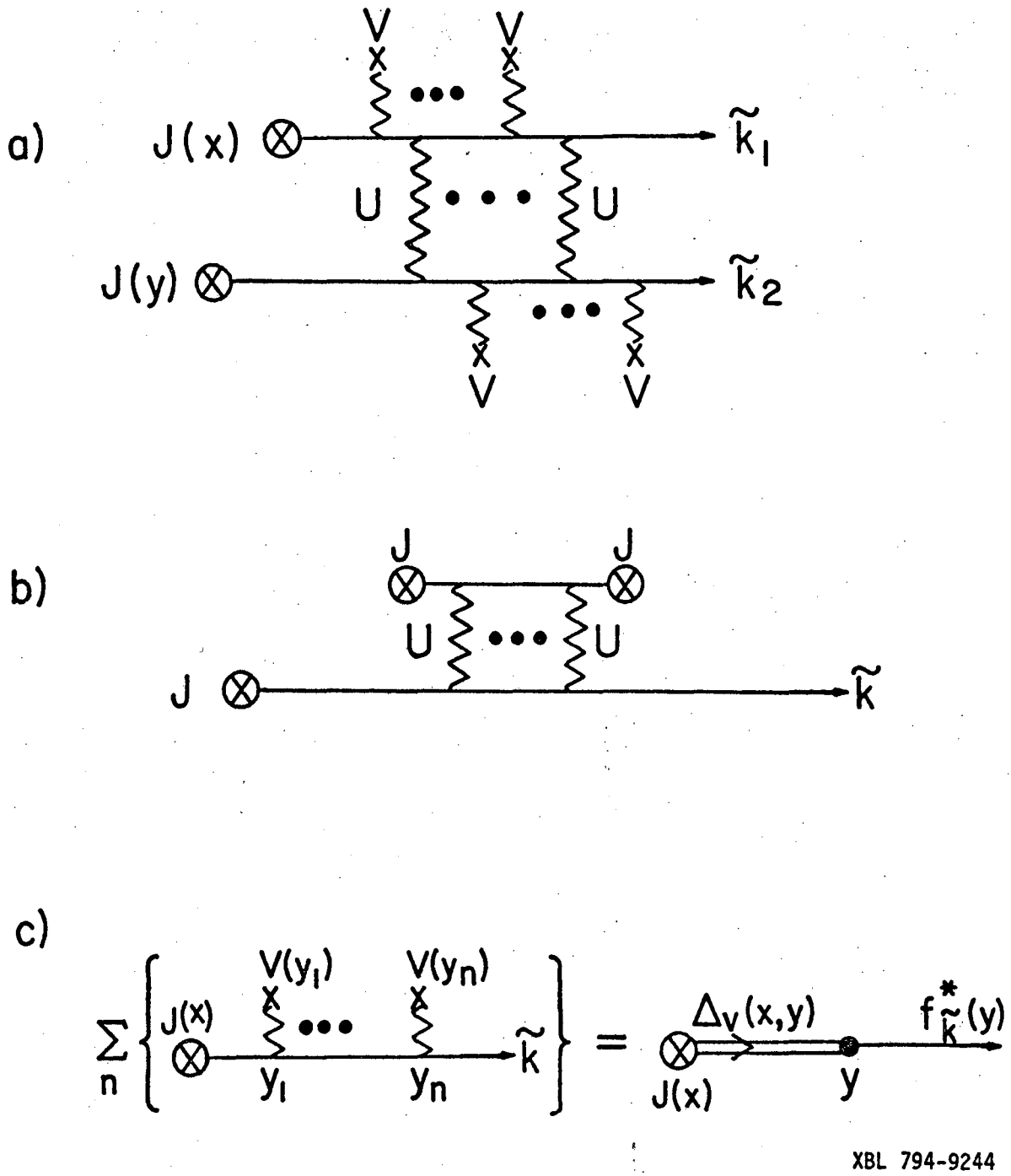
a)
V
V
J(x)
$\tilde{k}_1$
U
U
J(y)
$\tilde{k}_2$
V
V
b)
J
J
U
U
J
$\tilde{k}$
c)
$\sum_n$
J(x)
$V(y_1)$
$V(y_n)$
y_1
y_n
$\tilde{k}$
=
$\Delta_V(x,y)$
$f^*_{\tilde{k}}(y)$
J(x)
y
XBL 794-9244

Fig. 4.

TECHNICAL INFORMATION DEPARTMENT
LAWRENCE BERKELEY LABORATORY
UNIVERSITY OF CALIFORNIA
BERKELEY, CALIFORNIA 94720